Total Synthesis of an Immunosuppressive Glycolipid, (*2S,3S,4R*)-1-*O*-(α-D-Galactosyl)-2- tetracosanoylamino-1,3,4-nonanetriol

Kenji Murata, Tetsuya Toba, Kyoko Nakanishi, Bitoku Takahashi, Takashi Yamamura, Sachiko Miyake, and Hirokazu Annoura

Daiichi Suntory Biomedical Research Co., Ltd., 1-1-1, Wakayamadai, Shimamoto-cho, Mishima-gun, Osaka 618-8513, Japan, and Department of Immunology, National Institute of Neuroscience, National Center for Neuroscience and Psychiatry, Tokyo 187-8502, Japan

The Journal of Organic Chemistry®

Reprinted from
Volume 70, Number 6, Pages 2398–2401

JOC Note

Total Synthesis of an Immunosuppressive Glycolipid, (2*S*,3*S*,4*R*)-1-*O*-(α-D-Galactosyl)-2-tetracosanoylamino-1,3,4-nonanetriol

Kenji Murata,† Tetsuya Toba,† Kyoko Nakanishi,† Bitoku Takahashi,† Takashi Yamamura,‡ Sachiko Miyake,‡ and Hirokazu Annoura*,†

Daiichi Suntory Biomedical Research Co., Ltd., 1-1-1, Wakayamadai, Shimamoto-cho, Mishima-gun, Osaka 618-8513, Japan, and Department of Immunology, National Institute of Neuroscience, National Center for Neuroscience and Psychiatry, Tokyo 187-8502, Japan

hirokazu_annoura@dsup.co.jp

Received October 20, 2004

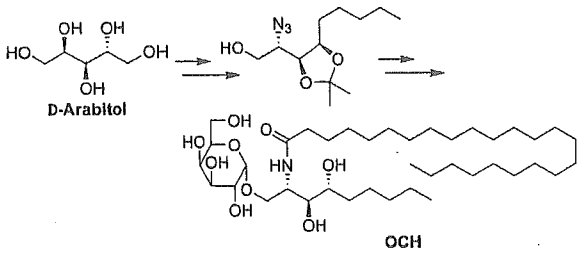

A practical and efficient total synthesis of (2*S*,3*S*,4*R*)-1-*O*-(α-D-galactosyl)-2-tetracosanoylamino-1,3,4-nonanetriol, OCH **1b**, a potential therapeutic candidate for Th1-mediated autoimmune diseases, is described. The synthesis incorporates direct alkylation onto epoxide **5** and stereospecific halide ion catalyzed α-glycosidation reaction. A key intermediate **10** was obtained in only eight steps and 37% overall yield from commercially available D-arabitol **2**, and the total synthesis of **1b** was accomplished in ~12 steps and 19% overall yield. This method will enable the synthesis of a variety of phytosphingolipids, especially that with the shorter sphingosine side chain than **1a**, in a highly stereoselective manner.

Natural killer (NK) T cells are potent producers of immunoregulatory cytokines and specific for glycolipid antigens bound by a nonpolymorphic major histocompatibility complex (MHC) class I-like molecule, CD1d.[1] The glycolipids, an α-galactosylceramide named KRN7000 **1a**[2] and an altered analogue, OCH **1b**,[3] possessing a shorter C5 sphingosine side chain, have been identified as NKT cell ligands (Figure 1). Whereas **1a** has been shown to cause both interferon (IFN)-γ and interleukin

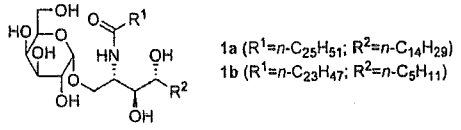

FIGURE 1. Structure of KRN7000 **1a** and OCH **1b**.

(IL)-4 production, **1b** induces a predominant production of IL-4, a key Th2 cytokine controlling autoimmunity. Compound **1b** is significantly effective in animal models of Th1-mediated autoimmune diseases such as experimental autoimmune encephalomyelitis (EAE) and collagen-induced arthritis (CIA), while **1a** showed only a minor effect.[3,4] It has recently been demonstrated that conversion of **1a** to its C-glycoside analogue leads to striking enhancement of activity on in vivo animal models of malaria and lung cancer.[5] Furthermore, similar substances including a tetraglycosylated glycolipid have recently been isolated from *Agelas Clathrodes*.[6] Consequently, considerable attention has been generated among synthetic chemists toward **1a**, **1b**, and their derivatives as new synthetic targets because of their distinctive biological and pharmacological properties as well as unique structural features. We present herein a practical and efficient total synthesis of immunosuppressive glycolipid **1b**.[7]

The significant structural difference between **1a** and **1b** is the length of a sphingosine side chain R^2. Reported procedures[2,8] for the syntheses of **1a** and its sphingosine derivatives, which essentially utilize Wittig-type or aldol-type reaction for the installation of the sphingosine side chain, gave low overall yields for **1b** and its analogues with a chain length shorter than C5 for R^2 and proved to be impractical.[9] Our strategy for resolving this problem is based upon the direct alkylation on epoxide **5**, which

* To whom correspondence should be addressed. Phone: +81-75-962-8188. Fax: +81-75-962-6448.
† Daiichi Suntory Biomedical Research Co., Ltd.
‡ National Institute of Neuroscience, NCNP.

(1) For reviews: (a) Porcelli, S. A.; Modlin, R. L. *Annu. Rev. Immunol.* **1999**, *17*, 297. (b) Hong, S.; Scherer, D. C.; Singh, N.; Mendiratta, S. K.; Serizawa, I.; Koezuka, Y.; Van Kaer, L. *Immunol. Rev.* **1999**, *169*, 31. (c) Sidobre, S.; Kronenberg, M. *J. Immunol. Methods* **2002**, *268*, 107. (d) Wilson, M. T.; Van Kaer, L. *Curr. Pharm. Des.* **2003**, *9*, 201. (e) Brigl, M.; Brenner, M. B. *Annu. Rev. Immunol.* **2004**, *22*, 817.

(2) (a) Morita, M.; Motoki, K.; Akimoto, K.; Natori, T.; Sakai, T.; Sawa, E.; Yamaji, K.; Koezuka, Y.; Kobayashi, E.; Fukushima, H. *J. Med. Chem.* **1995**, *38*, 2176. (b) Morita, M.; Sawa, E.; Yamaji, K.; Sakai, T.; Natori, T.; Koezuka, Y.; Fukushima, H.; Akimoto, K. *Biosci. Biotechnol. Biochem.* **1996**, *60*, 288. (c) Takikawa, H.; Muto, S.; Mori, K. *Tetrahedron* **1998**, *54*, 3141. (d) Graziani, A.; Passacantilli, P.; Piancatelli, G.; Tani, S. *Tetrahedron: Asymmetry* **2000**, *11*, 3921. (e) Plettenburg, O.; Bodmer-Narkevitch, V.; Wong C.-H. *J. Org. Chem.* **2002**, *67*, 4559.

(3) (a) Miyamoto, K.; Miyake, S.; Yamamura, T. *Nature* **2001**, *413*, 531. (b) Yamamura, T.; Miyake, S. PCT Int. Appl. WO 2003/016326, 2003; *Chem. Abstr.* **2003**, *138*, 205292m. (c) Yamamura, T.; Miyamoto, K.; Illes, Z.; Pal, E.; Araki, M.; Miyake, S. *Curr. Top. Med. Chem.* **2004**, *4*, 561. (d) Oki, S.; Chiba, A.; Yamamura, T.; Miyake, S. *J. Clin. Invest.* **2004**, *113*, 1631.

(4) Chiba, A.; Oki, S.; Miyamoto, K.; Hashimoto, H.; Yamamura, T.; Miyake, S. *Arthritis Rheum.* **2004**, *50*, 305.

(5) (a) Schmieg, J.; Yang, G.; Frank, R. W.; Tsuji, M. *J. Exp. Med.* **2003**, *198*, 1631. (b) Yang, G.; Schmieg, J.; Tsuji, M.; Frank, R. W. *Angew. Chem., Int. Ed.* **2004**, *43*, 3818.

(6) Costantino, V.; Fattorusso, E.; Imperatore, C.; Mangoni, A. *J. Org. Chem.* **2004**, *69*, 1174.

(7) Annoura, H.; Murata, K.; Yamamura, T. PCT Int. Appl. WO2004/072091, 2004; *Chem. Abstr.* **2004**, *141*, 225769n.

(8) (a) Schmidt, R. R., Maier, T. *Carbohydr. Res.* **1988**, *174*, 169. (b) Kobayashi, S.; Hayashi, T.; Kawasuji, T. *Tetrahedron Lett.* **1994**, *35*, 9573. (c) Azuma, H.; Tamagaki, S.; Ogino, K. *J. Org. Chem.* **2000**, *65*, 3538. (d) Fernandes, R. A.; Kumar, P. *Tetrahedron Lett.* **2000**, *41*, 10309. (e) Ndakala, J.; Hashemzadeh, M.; So, R. C.; Howell, A. R. *Org. Lett.* **2002**, *4*, 1719. (f) Ayad, T.; Génisson, Y.; Verdu, A.; Baltas, M.; Gorrichon, L. *Tetrahedron Lett.* **2003**, *44*, 579. (g) Lin, C.-C.; Fan, G.-T.; Fang, J.-M. *Tetrahedron Lett.* **2003**, *44*, 5281. (h) Chiu, H.-Yi; Tzou, D.-L. *J. Org. Chem.* **2003**, *68*, 5788.

10.1021/jo048151y CCC: $30.25
Published on Web 02/16/2005

SCHEME 1[a]

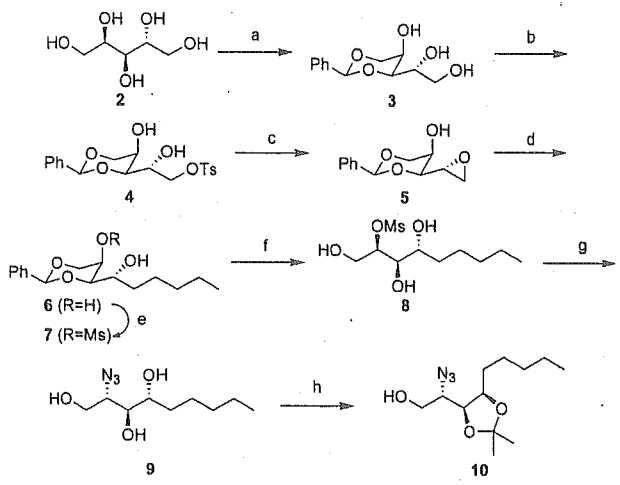

[a] Reagents and conditions: (a) PhCHO, dry HCl, rt, 91%; (b) *p*-TsCl, Et_3N, cat. Bu_2SnO, CH_2Cl_2, rt, quant; (c) *t*-BuOK, THF, rt, 91%; (d) *n*-Bu_2CuLi, THF, −40 °C, 98%; (e) MsCl, pyridine, −40 °C, 93%; (f) H_2, cat. $Pd(OH)_2$, EtOH, rt, quant; (g) NaN_3, DMF, 95 °C, 66%; (h) (i) cat. *p*-TsOH, 2,2-dimethoxypropane, rt; (ii) MeOH, rt, 75%.

has adequate stereocenters for the desired sphingosine side chain.[10]

Upon treatment of compound **3**,[11] which was readily prepared from D-arabitol **2** and benzaldehyde in 91% yield, with *p*-toluenesulfonyl chloride (*p*-TsCl) and triethylamine in the presence of a catalytic amount of dibutyltin oxide (Bu_2SnO),[12] regiospecific tosylation proceeded at the primary alcohol moiety to give **4** quantitatively (Scheme 1). The use of Bu_2SnO not only reduced the cost of this transformation but also greatly simplified the purification process since the yield was decreased to less than 30% when the reaction was carried out in the absence of Bu_2SnO. Treatment of **4** with *t*-BuOK produced the requisite epoxide **5** in 91% yield. Direct *n*-butylation onto **5** using organocopper lithium reagent in THF at −40 to −20 °C afforded 1,3-*O*-benzylidene-1,2,3,4-nonanetetrol **6** in 98% yield as the single product. Regioselective mesylation of the axial-OH in **6** with 1 equiv of methanesulfonyl chloride (MsCl) in pyridine at −40 °C to room temperature afforded **7** in 93% yield.

SCHEME 2[a]

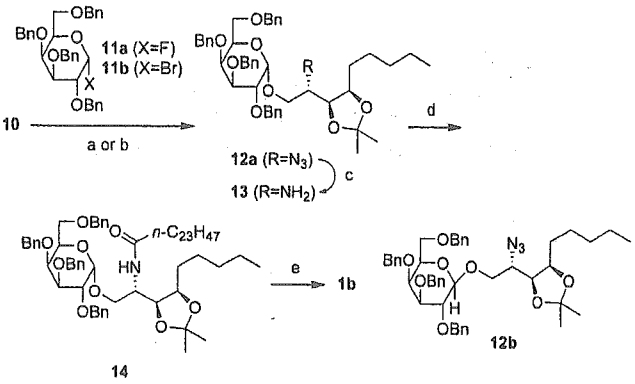

[a] Reagents and conditions: (a) **11a**, $BF_3{\cdot}Et_2O$, MS4Å, $CHCl_3$, −50 °C, 57% for **12a**, 25% for **12b**; (b) **11b**, *n*-Bu_4NBr, MS4Å, DMF−toluene (1:2.5), rt, 68% for **12a**; (c) H_2, Lindlar catalyst, EtOH, rt, quant; (d) *n*-$C_{23}H_{47}COOH$, EDCI, HOBt, *i*-Pr_2NEt, DMF−CH_2Cl_2 (1:3.5), 40 °C, 89%; (e) (i) HCl-dioxane, rt; (ii) H_2, cat. $Pd(OH)_2$, MeOH−$CHCl_3$ (3:1), rt, 84%

Deprotection of the benzylidene acetal in **7** by hydrogenation at atmospheric pressure in the presence of palladium hydroxide [$Pd(OH)_2$] in EtOH and subsequent azidation of **8** with sodium azide in DMF afforded **9** in 66% overall yield. Protection of the vicinal diols in **9** with a catalytic amount of *p*-toluenesulfonic acid (*p*-TsOH) in 2,2-dimethoxypropane at room temperature and quenching with MeOH afforded 3,4-isopropylidene acetal **10** in 75% yield.

As the key intermediate **10**, a glycosyl acceptor, was available, we next examined α-selective glycosidation reaction employing a variety of Lewis acids. After extensive experimentation, we found that glycosidation catalyzed by $BF_3{\cdot}Et_2O$ or *n*-Bu_4NBr with molecular sieves 4Å (MS4Å) worked well, but $AgClO_4$ reported for the synthesis[2] of **1a** gave only the undesired β-glycosylated product. Thus, treatment of **10** with benzyl protected galactosyl fluoride **11a** (1.8 equiv) in the presence of $BF_3{\cdot}Et_2O$ and MS4Å in $CHCl_3$ at −50 °C afforded α-galactosylceramide **12a** in 57% yield along with its β-isomer **12b** in 25% yield (Scheme 2). The stereochemistry of galactoside linkage was unambiguously determined by their NMR spectra[13] as well as conversion of **12a** into **1b** (vide infra). Surprisingly, when benzyl protected galactosyl bromide **11b**[14a] (1.8 equiv) and *n*-Bu_4NBr[14b] (3 equiv) with MS4Å were employed in toluene−DMF (2.5:1) at room temperature, **12a** was exclusively obtained in 68% yield. The corresponding β-galactosylated isomer **12b** could not be detected on TLC and NMR spectra. Upon using other ammonium bromides such as *n*-Hex_4NBr and Et_4NBr, the isolated yield of **12a** was decreased.

(9) According to the procedure reported in ref 2a, periodate oxidation of readily available tri-*O*-benzyl-D-galactose followed by Wittig-type reaction with a 5-fold molar excess of butylidene(triphenyl)phosphorane gave the desired (2*R*,3*S*,4*R*)-1,3,4-tri-*O*-benzyl-5-nonane-1,2,3,4-tetraol in less than 20% yield and consequently gave **1b** in low overall yield; see ref 3b. Also, when the more practical method for **1a** reported by Wong et al.[2e] was pursued for **1b**, similar Wittig reaction employing 3,4-di-*O*-benzyl-2-deoxy-6-*O*-triisopropylsilyl-D-galactopyranoside and propylidene(triphenyl)phosphorane resulted in complex mixtures containing an unavoidable byproduct in which the 3-benzyloxy group of galactopyranoside was eliminated. Therefore, our method is more efficient and practical for the synthesis of **1b** than those previously reported; however, this might not be the case for the synthesis of **1a**.

(10) During the preparation of this manuscript, Savage et al. have reported an alternative and efficient route for **1b**, although it requires the separation step of a 2:1 mixture of diastereomeric diols: Goff, R. D.; Gao, Y.; Mattner, J.; Zhou, D.; Yin, N.; Cantu, C., III; Teyton, L.; Bendelac, A.; Savage, P. B. *J. Am. Chem. Soc.* **2004**, *126*, 13602.

(11) (a) Hudson, C. S.; Hann, R. M.; Haskins, W. T. *J. Am. Chem. Soc.* **1943**, *65*, 1663. (b) Hough, L.; Theobald, R. S. *Methods Carbohydr. Chem.* **1963**, *1*, 94. (c) Dew, K. N.; Church, T. J.; Basu, B.; Vuorinen, T.; Serianni, A. S. *Carbohydr. Res.* **1996**, *284*, 135.

(12) Martinelli, M. J.; Nayyar, N. K.; Moher, E. D.; Dhokte, U. P.; Pawlak, J. M.; Vaidyanathan, R. *Org. Lett.* **1999**, *1*, 447.

(13) In the ^{13}C NMR (100 MHz, $CDCl_3$), the signal attributable to the anomeric carbon of **12a** appeared at δ 99.3, whereas that of **12b** was at δ 104.1. For ^{13}C NMR of glycosides: Pretsch, E.; Buhlmann, P.; Affolter, C. In *Structure Determination of Organic Compounds*, 3rd ed.; Springer-Verlag: 2000; pp 152−153. Also, in the ^1H NMR (400 MHz, $CDCl_3/CD_3OD$ 3:1) of **1b** derived from **12a**, the signal assignable to the hydrogen on the anomeric position was at δ 4.71 (d, 1H, $J = 3.8$ Hz), showing α-glycosidation product.

(14) Halide ion catalyzed glycosidation reaction was reported for the synthesis of α-linked disaccharide: (a) Spohr, U.; Le, N.; Ling, C.-C.; Lemieux, R. U. *Can. J. Chem.* **2001**, *79*, 238. (b) Lemieux, R. U.; Hendriks, K. B.; Stick, R. V.; James, K. *J. Am. Chem. Soc.* **1975**, *97*, 4056. Similar glycosidation methodology although in lower yield was reported: (c) Vo-Hoang, Y.; Micouin, L.; Ronet, C.; Gachelin, G.; Bonin, M. *ChemBioChem* **2003**, *4*, 27.

Selective reduction of the azido group of **12a** was achieved by hydrogenation with Lindlar catalyst in EtOH at room temperature to give amine **13** quantitatively. Compound **13** was acylated with *n*-tetracosanoic acid in the presence of 1-[3-(dimethylamino)propyl]-3-ethylcarbodiimide hydrochloride (EDCI), 1-hydroxybenzotriazole (HOBt) and *N,N*-diisopropylethylamine (*i*-Pr_2NEt) at 40 °C in DMF–CH_2Cl_2 (1:3.5) to afford amide **14** in 89% yield. Finally, deprotection of the isopropylidene acetal of **14** under acidic conditions and subsequent removal of the benzyl groups by hydrogenation with $Pd(OH)_2$ in MeOH–$CHCl_3$ (3:1) at room temperature furnished **1b** in 84% yield. The synthetic sample displayed satisfactory ^1H and ^{13}C NMR spectra, FABMS, and elemental analysis [mp 142–145 °C (recrystalized from EtOH/H_2O), $[\alpha]^{30}_D$ +53.9 (*c* 0.5, pyridine)].

In conclusion, we have developed an efficient and practical protocol for the synthesis of **1b** involving 12 steps starting from commercially available D-arabitol **2** in 19% overall yield. The key intermediate **10** as a glycosyl acceptor was obtained in only eight steps and 37% overall yield. Our method, amenable for large-scale synthesis, can provide a dozen grams of **1b** and enables the synthesis of a variety of phytosphingolipids related to **1a** and **1b**, especially those with the shorter sphingosine side chain or substituents other than aliphatic alkyl groups, in a highly stereoselective manner. The synthesis and structure–activity relationships of this series of compounds will be reported elsewhere in due course.[7]

Experimental Section

1,3-*O*-Benzylidene-D-arabitol (3). According to the reported procedures,[11] dry HCl was slowly bubbled into a mixture of D-arabitol **2** (98.8 g, 649 mmol) and benzaldehyde (78.8 mL, 775 mmol) for 15 min at room temperature. The mixture was allowed to stand at room temperature for 18 h. The resulting solid crystalline mass was broken up and placed in an evacuated desiccator containing KOH and H_2SO_4 for 24 h. The mass was triturated with Et_2O, neutralized with sat. $NaHCO_3$ aq., and filtered and washed with H_2O until the pH of the filtrate was neutral. The product was washed with Et_2O and recrystallized from 2-PrOH containing 0.5% v/v NH_4OH to give **3** (142.2 g, 91% yield) as colorless crystals; mp 130–131 °C; ^1H NMR (CD_3OD) δ 7.51–7.30 (m, 5H), 5.58 (s, 1H), 4.18 (d, 1H, J = 12 Hz), 4.11 (d, 1H, J = 12 Hz), 3.87–3.28 (m, 5H); HRMS calcd for $C_{12}H_{17}O_5$ $[M + H]^+$ 241.1076, found 241.1086.

1,3-*O*-Benzylidene-5-*O*-toluenesulfonyl-D-arabitol (4). To a suspension of **3** (34.0 g, 141 mmol) in CH_2Cl_2 (1200 mL) were added *p*-toluenesulfonyl chloride (27.0 g, 141 mmol), triethylamine (19.7 mL, 141 mmol) and dibutyltinoxide (702 mg, 2.82 mmol) at 0 °C. After being stirred for 21 h at room temperature, the mixture was concentrated in vacuo. The obtained residue was purified by column chromatography (CH_2Cl_2/MeOH 20:1) to give **4** (55.3 g, quant) as a white solid: ^1H NMR (DMSO-d_6) δ 7.73 (d, 2H, J = 8.2 Hz), 7.37–7.24 (m, 7H), 5.43 (s, 1H), 5.34 (d, 1H, J = 6.1 Hz), 4.77 (d, 1H, J = 6.5 Hz), 4.11 (dd, 1H, J = 9.8, 1.9 Hz), 4.04–3.85 (m, 4H), 3.71 (d, 1H, J = 9.2 Hz), 3.59 (d, 1H, J = 5.7 Hz), 2.32 (s, 3H); ^{13}C NMR ($CDCl_3$) δ 145.1, 137.3, 132.5, 129.9, 129.1, 128.2, 128.0, 125.8, 101.0, 77.9, 72.4, 70.9, 67.6, 62.7, 21.6; MS-ESI (*m/z*) 395 $[M + H]^+$; HRMS–FAB (*m/z*) $[M + H]^+$ calcd for $C_{19}H_{23}O_7S$, 395.1164, found 395.1189.

4,5-Anhydro-1,3-*O*-benzylidene-D-arabitol (5). To a solution of **4** (51.1 g, 130 mmol) in dry THF (800 mL) was added potassium *tert*-butoxide (18.1 g, 161 mmol) at 0 °C. The reaction mixture was stirred for 38 h at room temperature and then quenched with water. After being extracted with ethyl acetate, the organic layer was washed with brine, dried over anhydrous Na_2SO_4, and concentrated in vacuo. The residue was purified by column chromatography (*n*-hexane/EtOAc 1:1) to give **5** (26.2 g, 91%) as a white solid: ^1H NMR ($CDCl_3$) δ 7.52–7.34 (m, 5H), 5.57 (s, 1H), 4.25 (dd, 1H, J = 12, 1.8 Hz), 4.08 (dd, 1H, J = 12, 1.2 Hz), 3.78–3.75 (m, 2H), 3.35–3.31 (m, 1H), 2.93–2.84 (m, 3H); ^{13}C NMR ($CDCl_3$) δ 137.4, 129.3, 128.4, 126.0, 101.4, 79.7, 72.3, 64.4, 50.8, 45.9; MS-ESI (*m/z*) 223 $[M + H]^+$; HRMS–FAB (*m/z*) $[M + H]^+$ calcd for $C_{12}H_{15}O_4$, 223.0971, found 223.0895.

(2*R*,3*S*,4*R*)-1,3-*O*-Benzylidene-1,2,3,4-nonanetetrol (6). To a suspension of cupper iodide (I) (42.9 g, 225 mmol) in dry THF (560 mL) was added dropwise a solution of *n*-butyllithium (341 mL, 900 mmol, 2.64 M in hexane) at −40 °C under a nitrogen atmosphere. The reaction mixture was stirred for 30 min at −30 °C and then a solution of epoxide **5** (50.0 g, 225 mmol) in dry THF (400 mL) was added dropwise at −40 °C. After being stirred for 3 h at −20 °C, sat. $NaHCO_3$ aq. was added and the product was extracted with EtOAc. The organic layer was washed with brine, dried over anhydrous $MgSO_4$, and concentrated in vacuo to give **6** (61.7 g, 98%) as a white solid: ^1H NMR ($CDCl_3$) δ 7.52–7.50 (m, 2H), 7.42–7.38 (m, 3H), 5.60 (s, 1H), 4.28 (dd, 1H, J = 12, 1.8 Hz), 4.05 (1H, dd, J = 12, 1.3 Hz), 3.95–3.88 (m, 2H), 3.71 (dd, 1H, J = 6.6, 1.3 Hz), 3.25 (d, 1H, J = 8.7 Hz), 2.34 (d, 1H, J = 4.5 Hz), 1.73–1.53 (m, 2H), 1.40–1.30 (m, 6H), 0.90 (t, 3H, J = 6.7 Hz); ^{13}C NMR ($CDCl_3$) δ 129.1, 128.3, 126.0, 105.0, 101.2, 81.3, 72.6, 71.2, 63.8, 32.8, 31.8, 25.2, 22.6, 14.0; MS–FAB (*m/z*) 281 $[M + H]^+$; HRMS–FAB (*m/z*) $[M + H]^+$ calcd for $C_{16}H_{25}O_4$, 281.1753, found 281.1658.

(2*R*,3*S*,4*R*)-1,3-*O*-Benzylidene-2-*O*-methanesulfonyl-1,2,3,4-nonanetetrol (7). To a solution of **6** (3.90 g, 13.9 mmol) in dry pyridine (142 mL) was added methansulfonyl chloride (1.05 mL) at −40 °C under a nitrogen atmosphere. The mixture was stirred at the same temperature for 5 h and then gradually warmed to room temperature over 16 h. Azeotropic removal of pyridine by using toluene twice gave a residue that was subjected to column chromatography (*n*-hexane/EtOAc 3:2) to give **7** (4.65 g, 93%) as a white solid: ^1H NMR ($CDCl_3$) δ 7.51–7.48 (m, 2H), 7.42–7.35 (m, 3H), 5.59 (s, 1H), 4.99 (d, 1H, J = 1.4 Hz), 4.53 (dd, 1H, J = 13, 1.6 Hz), 4.18 (dd, 1H, J = 13, 1.1 Hz), 3.84–3.75 (m, 2H), 3.19 (s, 3H), 1.60–1.27 (m, 8H), 0.90 (t, 3H, J = 6.8 Hz); ^{13}C NMR (CDCl3) δ 129.3, 128.4, 126.1, 101.1, 80.9, 70.4, 70.0, 68.7, 38.7, 33.0, 32.0, 25.1, 22.8, 14.2; MS–FAB (*m/z*) 359 $[M + H]^+$; HRMS–FAB (*m/z*) $[M + H]^+$ calcd for $C_{17}H_{27}O_6S$, 359.1528, found 359.1448.

(2*R*,3*S*,4*R*)-2-*O*-Methanesulfonyl-1,2,3,4-nonanetetrol (8). To a solution of **7** (87.0 mg, 242 μmol) in EtOH (5.0 mL) was added palladium hydroxide ($Pd(OH)_2$) (45 mg). After hydrogenation of the mixture for 16 h at atmospheric pressure, the catalyst was filtered off and the filtrate was concentrated in vacuo to give **8** (65.7 mg, quant) as a white solid: ^1H NMR ($CDCl_3$) δ 5.03–5.00 (m, 1H), 4.02–4.00 (m, 2H), 3.62–3.60 (m, 2H), 3.19 (s, 3H), 1.76–1.72 (m, 1H), 1.56–1.28 (m, 7H), 0.90 (t, 3H, J = 6.7 Hz); ^{13}C NMR (CD_3OD) δ 83.8, 74.1, 71.3, 62.6, 38.6, 34.6, 33.2, 26.1, 23.8, 14.4; MS-ESI (*m/z*) 293 $[M + Na]^+$; HRMS–FAB (*m/z*) $[M - OH]^+$ calcd for $C_{10}H_{21}O_5S$, 253.1110, found 253.1069.

(2*S*,3*S*,4*R*)-2-Azido-1,3,4-nonanetriol (9). To a solution of **8** (36.9 mg, 136 μmol) in dry DMF (1.0 mL) was added NaN_3 (17.7 mg, 272 μmol) under a nitrogen atmosphere. The mixture was stirred for 3 h at 95 °C and then quenched with water. After being extracted with ethyl acetate, the organic layer was washed with brine twice, dried over anhydrous Na_2SO_4, and concentrated in vacuo. The residue was purified by column chromatography (CH_2Cl_2/MeOH 15:1) to give **9** (19.5 mg, 66%) as a white solid: ^1H NMR ($CDCl_3$) δ 4.05–3.98 (m, 1H), 3.91–3.74 (m, 3H), 3.71–3.66 (m, 1H), 2.67 (brs 1H), 2.52 (d, 1H, J = 4.4 Hz), 2.20 (brs, 1H), 1.61–1.52 (m, 2H), 1.40–1.31 (m, 6H), 0.91 (t, 3H, J = 6.6 Hz); ^{13}C NMR ($CDCl_3$) δ 74.8, 72.7, 63.3, 61.9, 32.0, 31.9, 25.6, 22.7, 14.2; MS–FAB (*m/z*) 218 $[M + H]^+$; HRMS–FAB (*m/z*) $[M + H]^+$ calcd for $C_9H_{20}N_3O_3$, 218.1505, found 218.1469.

(2*S*,3*S*,4*R*)-2-Azido-3,4-*O*-isopropylidene-1,3,4-nonanetriol (10). To a solution of **9** (4.00 g, 18.4 mmol) in dimethoxypropane (73 mL) was added a catalytic amount of *p*-toluenesulfonic acid monohydrate (175 mg, 92 μmol) at 0 °C. Stirring was continued for 2 h at room temperature. The mixture was

quenched with MeOH and then stirred for 1 h at room temperature. Removal of the solvent gave a residue, which was purified by column chromatography (*n*-hexane/EtOAc 4:1) to give **10** (3.61 g, 75%) as a colorless oil: ^{1}H NMR ($CDCl_3$) δ 4.21−4.16 (m, 1H), 4.02−3.95 (m, 2H), 3.90−3.84 (m, 1H), 3.50−3.45 (m, 1H), 2.11 (t, 1H, J = 5.6 Hz), 1.63−1.54 (m, 2H), 1.43 (s, 3H), 1.40−1.34 (m, 9H), 0.91(t, 3H, J = 6.9 Hz); ^{13}C NMR ($CDCl_3$) δ 108.6, 77.8, 76.6, 63.9, 61.2, 31.8, 29.4, 28.0, 26.2, 25.6, 22.6, 14.0; MS-ESI (*m/z*) 280 [M + Na]$^+$; HRMS−FAB (*m/z*) [M + H]$^+$ calcd for $C_{12}H_{24}N_3O_3$, 258.1818, found 258.1737.

(2*S*,3*S*,4*R*)-2-Azido-3,4-*O*-isopropylidene-1-*O*-(2,3,4,6-tetra-*O*-benzyl-α-D-galactosyl)-1,3,4-nonanetriol (12a). To a suspension of **10** (100 mg, 389 μmol), **11b** (428 mg, 710 μmol), and molecular sieves 4Å (powder, 340 mg) in dry toluene (3.4 mL) and dry DMF (1.4 mL) was added tetra-*n*-butylammonium bromide (*n*-Bu_4NBr) (377 mg, 1.17 mmol) under a nitrogen atmosphere. The reaction mixture was stirred for 5 days at room temperature. The mixture was quenched with MeOH (0.1 mL) and stirred for 1 h at room temperature. After being passed through Celite, the filtrate was washed with sat. $NaHCO_3$ aq. and brine and then dried over anhydrous $MgSO_4$. Removal of the solvent gave a residue, which was purified by column chromatography (*n*-hexane/EtOAc 7:1) to give **12a** (206 mg, 68%) as a colorless oil: ^{1}H NMR ($CDCl_3$) δ 7.40−7.26 (m, 20H), 4.97−4.93 (m, 2H), 4.87−4.79 (m, 2H), 4.74−4.70 (m, 2H), 4.57 (d, 1H, J = 12 Hz), 4.49 (d, 1H, J = 12 Hz), 4.41 (d, 1H, J = 12 Hz), 4.10−3.94 (m, 7H), 3.75−3.70 (m, 1H), 3.56−3.44 (m, 3H), 1.62−1.49 (m, 2H), 1.40−1.26 (m, 12H), 0.91 (t, 3H, J = 6.6 Hz); ^{13}C NMR ($CDCl_3$) δ 139.3, 139.1, 138.5, 128.8, 128.8, 128.7, 128.7, 128.7, 128.2, 128.1, 128.1, 128.0, 127.9, 108.6, 99.3, 79.1, 78.2, 77.0, 75.8, 75.7, 75.2, 73.9, 73.8, 73.3, 70.3, 70.0, 69.6, 60.3, 32.3, 29.7, 28.6, 26.7, 26.2, 23.0, 14.5; MS-ESI (*m/z*) 803 [M + Na]$^+$; HRMS−FAB (*m/z*) [M − N_2]$^+$ calcd for $C_{46}H_{57}NO_8$, 751.4084, found 751.4134.

(2*S*,3*S*,4*R*)-2-Azido-3,4-*O*-isopropylidene-1-*O*-(2,3,4,6-tetra-*O*-benzyl-β-D-galactosyl)-1,3,4-nonanetriol (12b). To a suspension of **10** (100 mg, 389 μmol), **11a** (285 mg, 524 μmol), and molecular sieves 4Å (powder, 400 mg) in dry $CHCl_3$ (5 mL) was added BF_3·Et_2O (47 μL, 368 μmol) in dry $CHCl_3$ (2 mL) at −50 °C under a nitrogen atmosphere. After stirring was continued for 14 h at the same temperature, the workup in the same manner for the reaction of **10** and **11b** provided **12a** (173 mg, 57%) along with **12b** (76 mg, 25%) as a colorless oil. **Data for 12b**: ^{1}H NMR ($CDCl_3$) δ 7.38−7.23 (m, 20H), 4.96−4.90 (m, 2H), 4.83−4.61 (m, 4H), 4.46−4.39 (m, 3H), 4.12−4.04 (m, 2H), 3.92−3.77 (m, 4H), 3.62−3.51 (m, 5H), 1.64−1.23 (m, 14H), 0.91 (t, 3H, J = 6.3 Hz); ^{13}C NMR ($CDCl_3$) δ 138.9, 138.6, 138.5, 137.9, 128.5, 128.4, 128.3, 128.3, 128.2, 128.0, 127.9, 127.8, 127.6, 127.6, 127.6, 108.3, 104.1, 82.2, 79.7, 77.8, 75.8, 75.3, 74.6, 73.6, 73.6, 73.5, 73.1, 70.6, 68.7, 60.5, 31.9, 29.4, 28.2, 26.1, 25.7, 22.6, 14.1; MS-ESI (*m/z*) 803 [M + Na]$^+$; HRMS−FAB (*m/z*) [M − N_2]$^+$ calcd for $C_{46}H_{57}NO_8$, 751.4084, found 751.4005.

(2*S*,3*S*,4*R*)-2-Amino-3,4-*O*-isopropylidene-1-*O*-(2,3,4,6-tetra-*O*-benzyl-α-D-galactosyl)-1,3,4-nonanetriol (13). To a solution of **12a** (2.58 g, 3.31 mmol) in EtOH (260 mL) was added palladium on calcium carbonate poisoned with lead (Lindlar catalyst) (2.60 g). After hydrogenation was carried out for 16 h at atmospheric pressure, the catalyst was filtered off and the filtrate was concentrated in vacuo to give **13** (2.46 g, quant) as a colorless oil: ^{1}H NMR ($CDCl_3$) δ 7.40−7.25 (m, 20H), 4.96−4.92 (m, 2H), 4.84−4.64 (m, 4H), 4.58 (d, 1H, J = 11 Hz), 4.50 (d, 1H, J = 12 Hz), 4.41 (d, 1H, J = 12 Hz), 4.13−3.86 (m, 6H), 3.58−3.51 (m, 2H), 3.42−3.37 (m, 1H), 3.07−3.01 (m, 1H), 1.65−1.20 (m, 14H), 0.90 (t, 3H, J = 5.6 Hz); ^{13}C NMR ($CDCl_3$) δ 138.8, 138.7, 138.6, 138.0, 128.4, 128.4, 128.2, 127.8, 127.8, 127.7, 127.6, 127.6, 127.5, 127.4, 107.9, 99.0, 79.1, 79.0, 77.9, 74.9, 74.8, 73.5, 73.3, 73.0, 72.4, 69.5, 69.0, 50.7, 31.9, 29.8, 28.3, 26.0, 25.9, 22.6, 14.1; MS-ESI (*m/z*) 754 [M + H]$^+$; HRMS−FAB (*m/z*) [M + H]$^+$ calcd for $C_{46}H_{60}NO_8$, 754.4319, found 754.4194.

(2*S*,3*S*,4*R*)-3,4-*O*-Isopropylidene-1-*O*-(2,3,4,6-tetra-*O*-benzyl-α-D-galactosyl)-2-tetracosanoylamino-1,3,4-nonanetriol (14). To a suspension of *n*-tetracosanoic acid (1.22 g, 3.31 mmol) in DMF (90 mL) and CH_2Cl_2 (210 mL) were added 1-ethyl-3-(3-dimethylaminopropyl) carbodiimide hydrochloride (EDCI) (761 mg, 3.97 mmol) and 1-hydroxybenzotriazol (HOBt) (536 mg, 3.97 mmol) at 0 °C. After the mixture was stirred for 30 min at room temperature, **13** (2.46 g, 3.26 mmol) and *i*-Pr_2NEt (1.38 mL, 7.97 mmol) in CH_2Cl_2 (120 mL) were added and stirred for 16 h at 30 °C. The mixture was diluted with EtOAc/Et_2O (4:1) and sat. $NaHCO_3$ aq., and then the organic layer was separated and washed with 1 M HCl aq. and brine, and dried over anhydrous $MgSO_4$. Removal of the solvent gave a residue, which was purified by column chromatography (*n*-hexane/EtOAc 3:1) to give **14** (3.25 g, 89%) as a white solid: ^{1}H NMR ($CDCl_3$) δ 7.41−7.24 (m, 20H), 6.28 (d, 1H, J = 8.4 Hz), 4.95−4.90 (m, 2H), 4.83−4.73 (m, 2H), 4.75 (d, 1H, J = 12 Hz), 4.66 (d, 1H, J = 11 Hz), 4.58 (d, 1H, J = 12 Hz), 4.49 (d, 1H, J = 12 Hz), 4.38 (d, 1H, J = 12 Hz), 4.13−4.03 (m, 4H), 3.98 (t, 1H, J = 6.2 Hz), 3.93−3.90 (m, 3H), 3.69−3.53 (m, 2H), 3.39 (dd, 1H, J = 9.4, 5.7 Hz), 2.08−1.95 (m, 2H), 1.55−1.25 (m, 50H), 1.40 (s, 3H), 1.32 (s, 3H), 0.90−0.84 (m, 6H); ^{13}C NMR ($CDCl_3$) δ 172.4, 138.7, 138.4, 137.6, 128.5, 128.4, 128.4, 128.4, 128.3, 128.0, 127.9, 127.8, 127.7, 127.6, 127.5, 107.8, 99.9, 79.0, 77.8, 76.8, 75.5, 74.8, 74.7, 73.6, 73.5, 73.0, 70.8, 69.9, 69.6, 48.7, 36.8, 31.9, 31.8, 29.7, 29.7, 29.6, 29.5, 29.4, 29.3, 28.9, 28.2, 26.2, 26.0, 25.7, 22.7, 22.6, 14.1, 14.1; MS−FAB 1105 [M + H]$^+$; HRMS−FAB (*m/z*) [M + H]$^+$ calcd for $C_{70}H_{106}NO_9$, 1104.7868, found 1104.7589.

(2*S*,3*S*,4*R*)-1-*O*-(α-D-Galactosyl)-2-tetracosanoylamino-1,3,4-nonanetriol (1b). To a solution of **14** (89 mg, 81 μmol) in MeOH (1.0 mL) and CH_2Cl_2 (5.0 mL) was added 4 M HCl aq. in dioxane (100 μL) at 0 °C. After the mixture was stirred for 2 h at room temperature, evaporation of the solvent gave a residue, which was purified by column chromatography (CH_2Cl_2/MeOH 30:1) to give the product by which the acetal group was deprotected. To a solution of the obtained diol in MeOH (3.0 mL) and $CHCl_3$ (1.0 mL) was added $Pd(OH)_2$ (25 mg). After hydrogenation was carried out for 3 h at atmospheric pressure, the catalyst was filtered off and the filtrate was evaporated to give **1b** (46 mg, 84%) as colorless crystals, mp 142−145 °C (recrystallized from EtOH/H_2O 10:1); $[\alpha]^{30}_D$ +53.9 (*c* 0.5, pyridine); ^{1}H NMR ($CDCl_3$/CD_3OD 3:1) δ 4.71 (d, 1H, J = 3.8 Hz), 4.01−3.98 (m, 1H), 3.74−3.65 (m, 2H), 3.62−3.45 (m, 6H), 3.35−3.31 (m, 2H), 2.00 (t, 2H, J = 7.6 Hz), 1.51−1.01 (m, 50H), 0.71−0.67 (m, 6H); ^{13}C NMR (pyridine-d_5) δ 173.8, 102.1, 77.3, 73.6, 73.0, 72.2, 71.6, 70.9, 69.2, 63.2, 52.0, 37.4, 34.9, 33.0, 32.7, 30.6, 30.6, 30.5, 30.4, 30.4, 30.3, 30.2, 27.0, 26.7, 23.6, 23.5, 14.8; MS−FAB (*m/z*) 704 [M + H]$^+$; HRMS−FAB (*m/z*) [M + H]$^+$ calcd for $C_{39}H_{78}NO_9$, 704.5677, found 704.5687. Anal. Calcd for $C_{39}H_{77}NO_9$·H_2O: C, 64.87; H, 11.03; N, 1.94. Found: C, 64.71; H, 10.88; N, 1.94.

Acknowledgment. We thank Mr. N. Takemoto, Ms. M. Akabane, Mr. N. Ogou, and Ms. J. Futamura for their contribution to the synthesis of related analogues. We also thank Drs. T. Nishihara and G. Nakayama for their support and encouragement throughout this study.

Note Added after ASAP Publication. As the result of a production error, the formatting of the compound names in the Experimental Section was inconsistent in the version published ASAP February 16, 2005. These have been corrected, and the solvent was changed in the synthesis of **12b**. The corrected version was published February 18, 2005.

Supporting Information Available: ^{1}H and/or ^{13}C NMR spectra of **1b**, **3**−**10**, **12a**, **12b**, **13**, and **14**. This material is available free of charge via the Internet at http://pubs.acs.org.

JO048151Y

Modulation of CD1d-restricted NKT cell responses by using *N*-acyl variants of α-galactosylceramides

Karl O. A. Yu*†, Jin S. Im*†, Alberto Molano*†, Yves Dutronc*‡, Petr A. Illarionov§, Claire Forestier*, Nagatoshi Fujiwara*¶, Isa Arias*, Sachiko Miyake‖, Takashi Yamamura‖, Young-Tae Chang**, Gurdyal S. Besra§, and Steven A. Porcelli*††

*Department of Microbiology and Immunology, Albert Einstein College of Medicine, 1300 Morris Park Avenue, Bronx, NY 10461; §School of Biosciences, University of Birmingham, Edgbaston, Birmingham B15 2TT, United Kingdom; ‖Department of Immunology, National Institute of Neuroscience, National Center of Neurology and Psychiatry, 4-1-1 Ogawahigashi, Kodaira, Tokyo 187-8502, Japan; and **Department of Chemistry, New York University, 29 Washington Place, New York, NY 10003

Edited by Douglas T. Fearon, University of Cambridge, Cambridge, United Kingdom, and approved January 18, 2005 (received for review October 8, 2004)

A form of α-galactosylceramide, KRN7000, activates CD1d-restricted Vα14-invariant (Vα14i) natural killer (NK) T cells and initiates multiple downstream immune reactions. We report that substituting the C26:0 *N*-acyl chain of KRN7000 with shorter, unsaturated fatty acids modifies the outcome of Vα14i NKT cell activation. One analogue containing a diunsaturated C20 fatty acid (C20:2) potently induced a T helper type 2-biased cytokine response, with diminished IFN-γ production and reduced Vα14i NKT cell expansion. C20:2 also exhibited less stringent requirements for loading onto CD1d than KRN7000, suggesting a mechanism for the immunomodulatory properties of this lipid. The differential cellular response elicited by this class of Vα14i NKT cell agonists may prove to be useful in immunotherapeutic applications.

cytokines | inflammation | autoimmunity | immunoregulation

Natural killer (NK) T cells were defined originally as lymphocytes coexpressing T cell receptors (TCRs) and C-type lectin receptors characteristic of NK cells. A major subset of NKT cells recognizes the MHC class I-like molecule CD1d by using TCRs composed of an invariant TCR-α chain (mouse Vα14-Jα18, human Vα24-Jα18) paired with TCR-β chains with markedly skewed Vβ usage (1). These CD1d-restricted Vα14-invariant (Vα14i) NKT cells are highly conserved in phenotype and function between mice and humans (2). Vα14i NKT cells influence various immune responses and play an important role in regulating autoimmunity (3, 4). One example is the nonobese diabetic mouse. When compared with normal mice, nonobese diabetic mice have fewer Vα14i NKT cells, which are defective in their capacity to produce antiinflammatory cytokines like IL-4 (5, 6). Deficiencies in NKT cells have also been observed in humans with various autoimmune diseases (7, 8).

Vα14i NKT cells have been manipulated to prevent or treat autoimmune disease, mostly through the use of KRN7000, a synthetic α-galactosylceramide (α-GalCer, Fig. 1*A*) that binds to the hydrophobic groove of CD1d and then activates Vα14i NKT cells by means of TCR recognition (9). KRN7000 treatment of nonobese diabetic mice blocks development of T helper (T_H) type 1-mediated autoimmune destruction of pancreatic islet β-cells, thus delaying or preventing disease (10–12). There has been considerable interest in methods that would allow a more selective activation of these cells. In particular, the ability to trigger IL-4 production without eliciting strong IFN-γ or other proinflammatory cytokines may reinforce the immunoregulatory functions of Vα14i NKT cells. This effect is detected after Vα14i NKT cell activation with a glycolipid designated OCH, which is an α-GalCer analogue that is structurally distinct from KRN7000 in having a substantially shorter sphingosine chain and functionally by its preferential induction of IL-4 secretion (13, 14).

In this study, we investigated responses to α-GalCer analogues produced by alteration of the length and extent of unsaturation of their *N*-acyl substituents. Such modifications altered the outcome of Vα14i NKT cell activation and, in some cases, led to a T_H2-biased and potentially antiinflammatory cytokine response. This change in the NKT cell response was likely the result of an alteration of downstream steps in the cascade of events triggered by Vα14i NKT cell activation, including the reduction of secondary activation of IFN-γ-producing NK cells. These findings point to a class of Vα14i NKT cell agonists that may have superior properties for the treatment of autoimmune and inflammatory diseases.

Materials and Methods

Mice and Cell Lines. C57BL/6 mice (8- to 15-wk-old females) were obtained either from The Jackson Laboratory or Taconic Farms. CD1d$^{-/-}$ mice were provided by M. Exley and S. Balk (Beth Israel–Deaconess Medical Center, Harvard Medical School, Boston) (15). Vα14i NKT cell-deficient Jα18$^{-/-}$ mice were a gift from M. Taniguchi and T. Nakayama (Chiba University, Chiba, Japan) (16). Both knockout mice were in the C57BL/6 background. Animals were kept in specific pathogen-free housing. The protocols that we used were in accordance with approved institutional guidelines.

Mouse CD1d-transfected RMA-S cells (RMA-S.mCD1d) were provided by S. Behar (Brigham and Women's Hospital, Harvard Medical School) (17). WT or cytoplasmic tail-deleted CD1d-transfected A20 cells and the Vα14i NKT hybridoma DN3A4–1.2 were provided by M. Kronenberg (La Jolla Institute for Allergy and Immunology, La Jolla, CA) (18, 19). Hybridoma DN32D3 was a gift from A. Bendelac (University of Chicago, Chicago) (1). Cells were cultured in RPMI medium 1640 (GIBCO) supplemented with 10% heat-inactivated FCS (Gemini Biological Products, Calabasas, CA)/10 mM Hepes/2 mM L-glutamine/0.1 mM nonessential amino acids/55 μM 2-mercaptoethanol/100 units/ml penicillin/100 μg/ml streptomycin (GIBCO) in a 37°C humidified incubator with 5% CO_2.

Glycolipids. BF1508-84 was synthesized by Biomira (Edmonton, Canada). OCH [(2*S*, 3*S*, 4*R*)-1-*O*-(α-D-galactopyranosyl)-*N*-tetracosanoyl-2 amino-1,3,4-nonanetriol] was synthesized as described (13). An overview of the methods for synthesis of KRN7000 [(2*S*, 3*S*, 4*R*)-1-*O*-(α-D-galactopyranosyl)-*N*-hexaco-

This paper was submitted directly (Track II) to the PNAS office

Abbreviations: Vα14i, Vα14 invariant; NK, natural killer; α GalCer, α galactosylceramide; T_H, T helper; TCR, T cell receptor; RMA S.mCD1d, mouse CD1d transfected RMA S cells.

†K.O.A.Y., J.S.I., and A.M. contributed equally to this work.

‡Present address: Department of Dermatology, Bocage Hospital, BP 77908, 21079 Dijon Cedex, France.

¶Present address: Department of Host Defense, Graduate School of Medicine, Osaka City University, 1-4-3 Asahi-machi, Abeno ku, Osaka 545-8585, Japan.

††To whom correspondence should be addressed. E-mail: porcelli@aecom.yu.edu.

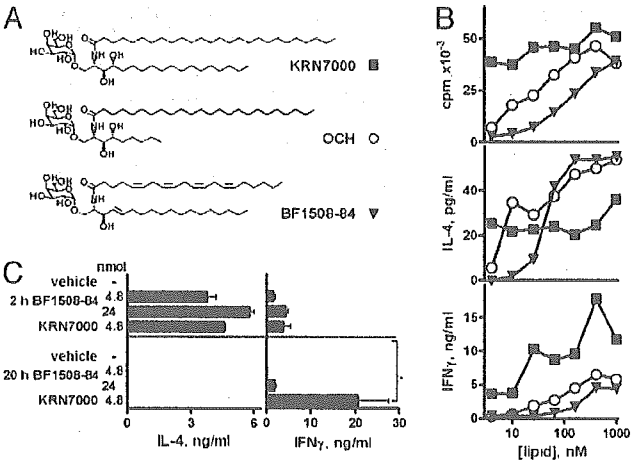

Fig. 1. Induction of a T_H2-polarized cytokine response by an unsaturated analogue of α-GalCer. (*A*) Glycolipid structures. (*B*) [^{3}H]thymidine incorporation and supernatant IL-4 and IFN-γ levels in 72-h splenocyte cultures with graded amounts of glycolipid. Means from triplicate cultures are shown; SEMs were typically < 10% of the mean. (*C*) Serum IL-4 and IFN-γ levels (at 2 and 20 h) of C57BL 6 mice injected i.p. with 4.8 or 24 nmol of glycolipid. KRN7000 was the only glycolipid that induced significant IFN-γ levels at 20 h (*, $P < 0.05$, Kruskall–Wallis test, Dunn's posttest). Means ± SD of two or three mice per group are shown.

sanoyl-2-amino-1,3,4-octadecanetriol] and other *N*-acyl analogues used in this study is shown in Fig. 7, which is published as supporting information on the PNAS web site. Lipids were dissolved in chloroform/methanol (2:1 ratio) and stored at −20°C. Aliquots from this stock were dried and reconstituted to either 100 μM in DMSO for *in vitro* work or to 500 μM in 0.5% Tween-20 in PBS for *in vivo* studies.

***In Vitro* Stimulations.** Bulk splenocytes were plated at 300,000 cells per well in 96-well flat-bottom tissue culture plates with glycolipid diluted in 200 μl of medium. After 48 or 72 h at 37°C, 150 μl of supernatant was removed for cytokine measurements, and 0.5 μCi (1 Ci = 37 GBq) [^{3}H]thymidine per well (specific activity 2 Ci/mmol; PerkinElmer) was added for an 18-h pulse. Proliferation was estimated by harvesting cells onto 96-well filter mats and counting β-scintillations with a 1450 Microbeta Trilux (Wallac, Gaithersburg, MD; PerkinElmer).

Supernatant levels of IL-2, IL-4, IL-12p70, and IFN-γ were measured by ELISA using capture and biotinylated detection antibody pairs (BD PharMingen) and streptavidin–horseradish peroxidase (Zymed) with TMB-Turbo substrate (Pierce) or streptavidin–alkaline phosphatase (Zymed) with 4-nitrophenyl phosphate substrate (Sigma). IL-2 standard was obtained from R & D Systems; IL-4, IL-12p70 and IFN-γ were obtained from PeproTech (Rocky Hill, NJ).

Hybridoma Stimulations. CD1d$^+$ RMA-S or A20 cells (50,000 cells in 100 μl per well) were pulsed with graded doses of glycolipid for 6 h at 37°C. After three washes in PBS, Vα14i NKT hybridoma cells (50,000 cells in 100 μl) were added for 12 h. Supernatant IL-2 was assayed by ELISA. Alternatively, CD1d-transfected cells (RMA-S.mCD1d) were lightly fixed either before or after exposure to antigen (20). Cells were washed twice in PBS and then fixed in 0.05% glutaraldehyde (grade I, Sigma) in PBS for 30 s at room temperature. Fixative was quenched by addition of 0.2 M L-lysine (pH 7.4) for 2 min, followed by two washes with medium before addition of responders.

For cell-free presentation, recombinant mouse CD1d (1 μg/ml in PBS) purified from a baculovirus expression system (21) was adhered to tissue culture plates for 1 h at 37°C. After the washing off of unbound protein, glycolipids were then added at varying concentrations for 1 h at 37°C. Lipids were added in a 150 mM NaCl/10 mM sodium phosphate buffer (pH 7) with or without 0.025% Triton X-100. Wells were washed before addition of hybridoma cells.

***In Vivo* Studies.** Mice were given i.p. injections of 4.8 nmol of glycolipid in 0.2 ml of PBS plus 0.025% Tween-20 or vehicle alone. Sera were collected and tested for IL-4, IL-12p70, and IFN-γ, as described above. Alternatively, mice were killed at various times for FACS analysis.

Flow Cytometry. Splenocytes or thymocytes were isolated and used without further purification. Nonspecific staining was blocked by using FACS buffer (0.1% BSA/0.05% NaN_3 in PBS) with 10 μg/ml rat anti-mouse CD16/32 (2.4G2; The American Type Culture Collection). Cells ($\leq 10^6$) were stained with phycoerythrin or allophycocyanin-conjugated glycolipid/mouse CD1d tetramers (21) for 30–90 min at room temperature and then with fluorescently labeled antibodies (from Caltag, South San Francisco, CA, or PharMingen) for 30 min at 4°C. Data were acquired on either a FACSCalibur or LSR-II flow cytometer (Becton Dickenson) and analyzed by using WINMDI 2.8 (Scripps Research Institute, La Jolla, CA). For some experiments, dead cells were excluded by using propidium iodide (Sigma) or 4′,6-diamidino-2-phenylindole (Roche).

FACS-based cytokine secretion assays (Miltenyi Biotec, Auburn, CA) were used to quantitatively detect single-cell production of IL-4 or IFN-γ. Splenocytes were aseptically collected from mice that were previously injected i.p. with glycolipid analogues and not subjected to further stimulation. When applicable, 10^6 cells were prestained with labeled tetramer for 30 min at room temperature and then washed in PBS plus 0.1% BSA. Cells were then stained with the cytokine catch reagent according to the manufacturer's instructions, followed by incubation with rotation in 2 ml of medium at 37°C for 45 min. Cells were then washed, stained with fluorescently labeled antibodies to cell-surface antigens, phycoerythrin-conjugated anti-IFN-γ or IL-4, and propidium iodide, as described above.

Results

T_H2-Skewing Properties of an α-GalCer Analogue. During screening of a panel of synthetic glycosyl ceramides, we identified a compound that showed T_H2-skewing of the cytokine profile generated by Vα14i NKT cell activation. Glycolipid BF1508-84 differed structurally from both OCH and KRN7000 by having a shortened, unsaturated fatty-acid chain (C20:4 arachidonate) and a double bond in place of the 4-hydroxy in the sphingosine base (Fig. 1*A*). Despite these modifications, BF1508-84 activated proliferation and cytokine secretion by mouse splenocytes (Fig. 1*B*). These responses were Vα14i NKT cell-dependent, as demonstrated by their absence in both CD1d$^{-/-}$ and Jα18$^{-/-}$ mice (data not shown). Maximal proliferation and IL-4 levels were comparable with those obtained with KRN7000 and OCH, although a higher concentration of BF1508-84 was required to reach similar responses. Interestingly, IFN-γ secretion stimulated by BF1508-84, even at higher tested concentrations, did not reach the levels seen with KRN7000. This profile of cytokine responses suggested that BF1508-84 can elicit a T_H2-biased Vα14i NKT cell-dependent cytokine production, similar to OCH (13).

We measured serum cytokine levels at various times after a single injection of either KRN7000 or BF1508-84 into C57BL/6 mice. Our studies confirm published reports that a single i.p. injection of KRN7000 leads to a rapid 2-h peak of serum IL-4 (Fig. 1*C* and data not shown). However, IFN-γ levels were relatively low at 2 h but rose to a plateau at 12–24 h (13, 22). With

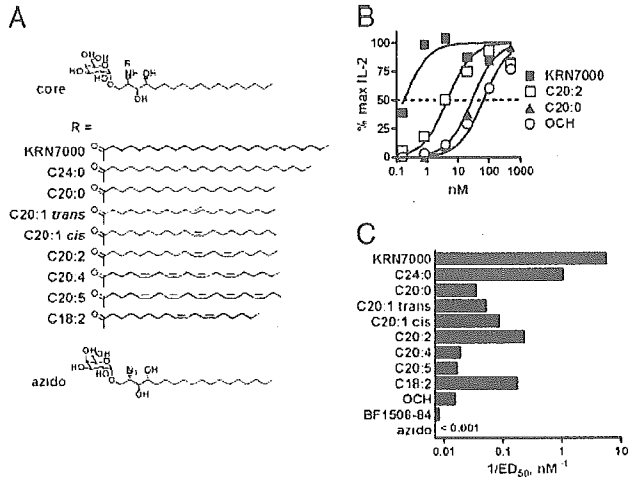

Fig. 2. Recognition of a panel of unsaturated analogues of KRN7000 by a canonical Vα14i NKT hybridoma. (*A*) Analogue structures. (*B*) Dose–response curves showing IL-2 production by hybridoma DN3A4–1.2 after stimulation with RMA-S.mCD1d cells pulsed with various doses of glycolipid. Maximal IL-2 concentrations in each assay were designated as 100%. Four-parameter logistic equation dose–response curves are shown; the dotted line denotes the half-maximal dose. (*C*) Relative potencies of the analogue panel in Vα14i NKT cell recognition, plotted as the reciprocal of the effective dose required to elicit a half-maximal response (1/ED_{50}). Similar results were obtained by using another Vα14i NKT hybridoma, DN32D3.

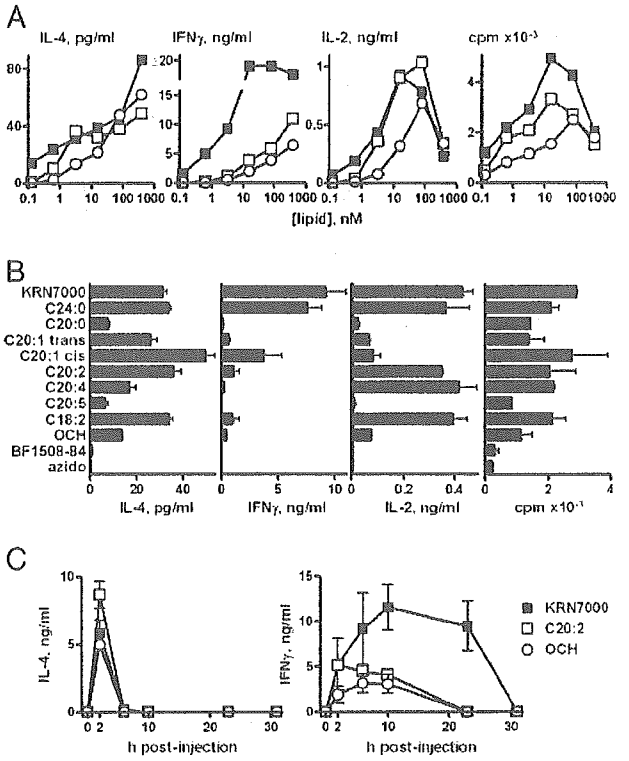

Fig. 3. T_H2-skewing of *in vitro* and *in vivo* cytokine responses to C20:2. (*A*) Dose–response curves reporting 48 h IL-4, IFN-γ, or IL-2 production, and cell proliferation of splenocytes in response to KRN7000, C20:2, and OCH. Means of duplicate cultures are shown; SEM were < 10% of the means. (*B*) Cytokine and proliferation measurements on splenocytes exposed to a submaximal dose (3.2 nM) of the panel of α-GalCer analogues shown in Fig. 2. Mean ± SEM from duplicate cultures shown. (*C*) Serum IL-4 and IFN-γ levels in mice given 4.8 nmol of KRN7000, C20:2, or OCH. Mean ± SD of two or three mice are shown. Vehicle-treated mice had cytokine levels below limits of detection. The results shown are representative of two or more experiments.

BF1508-84, production of IL-4 at 2 h was preserved, whereas IFN-γ was barely detectable at 20 h (Fig. 1*C*). This pattern was identical to that reported for OCH (13, 22) and was not due to the lower potency of BF1508-84 because a 5-fold greater dose did not change the T_H2-biased cytokine profile (Fig. 1*C*).

Systematic Variation of Fatty-Acyl Unsaturation in α-GalCer. The cytokine response to BF1508-84 suggested that altering the fatty-acid length and unsaturation of α-GalCer could provide an effective strategy for creating Vα14i NKT cell activators with modified functional properties. We used a synthetic approach (Fig. 7, and G.S.B. and P.A.I., unpublished data) to generate lipids in which 20-carbon acyl chains with varying degrees of unsaturation were coupled onto the α-galactosylated sphingosine core structure (Fig. 2*A*). These compounds were first screened for the ability to activate a canonical Vα14-Jα18/Vβ8.2$^+$, CD1d-restricted NKT cell hybridoma cocultured with CD1d$^+$ antigen-presenting cells. Hybridoma DN3A4–1.2 recognized all C20 analogues of α-GalCer with various potencies when presented by CD1d-transfected RMA-S cells, and it failed to recognize an azido-substituted analogue lacking a fatty-acid chain (Fig. 2 *B* and *C*). As reported (9), mere shortening of the fatty-acid chain affected Vα14i NKT cell recognition, and reduction of saturated fatty-acid length from C26 to C20 was associated with a ≈2 log decrease in potency. However, insertion of double bonds into the C20 acyl chain augmented stimulatory activity. One lipid in particular, with unsaturations at carbons 11 and 14 (C20:2), was more potent than other analogues in the panel. This increase in potency seemed to be a direct result of the two double bonds, because an independently synthesized analogue with a slightly shorter diunsaturated acyl chain (C18:2) showed a potency similar to that of C20:2 (Fig. 2*C*).

We also studied *in vitro* splenocyte cytokine polarization resulting from Vα14i NKT cell stimulation by each lipid in the panel. Supernatant IL-4, IFN-γ, and IL-2 levels were measured over a wide range of glycolipid concentrations. All C20 variants induced IL-4 production comparable with that of KRN7000 (Fig. 3 *A* and *B*, and data not shown). However, IFN-γ levels for all but one C20 analogue (C20:1 *cis*) were markedly reduced to one-fourth of the maximal levels observed with KRN7000 and the closely related C24:0 analogue, or less. In addition, C20:1-*cis*, C20:2, and C18:2 were unique in this class of compounds in inducing strong IL-2 production and cellular proliferation similar to that seen with KRN7000 and C24:0 yet with much lower IFN-γ induction. This *in vitro* T_H2-bias was also evident *in vivo*. Mice given C20:2 and C20:4 showed systemic cytokine production that resembled stimulation by OCH or BF1508-84. Thus, a rapid burst of serum IL-4 was observed without the delayed and sustained production of IFN-γ typical of KRN7000 (Fig. 3*C* and data not shown). No significant difference between the glycolipids was seen in serum IL-12p70 levels at 6 h after treatment (data not shown).

Identification of Cytokine-Producing Cells *in Vivo*. Previous reports (23–25) established that Vα14i NKT cells are a predominant source of IL-4 and IFN-γ in the early (2 h) response to KRN7000 and that by 6 h after injection these cells become progressively undetectable because of receptor down-modulation, whereas secondarily activated NK cells begin to actively produce IFN-γ. Gating on either α-GalCer-loaded CD1d tetramer$^+$ or NK1.1$^+$ T cells, we observed similar strong cytokine secretion for both IL-4 (data not shown) and IFN-γ in Vα14i NKT cells at 2 h after injection of KRN7000 or C20:2 (Fig. 4 *A* and *B*). We concluded

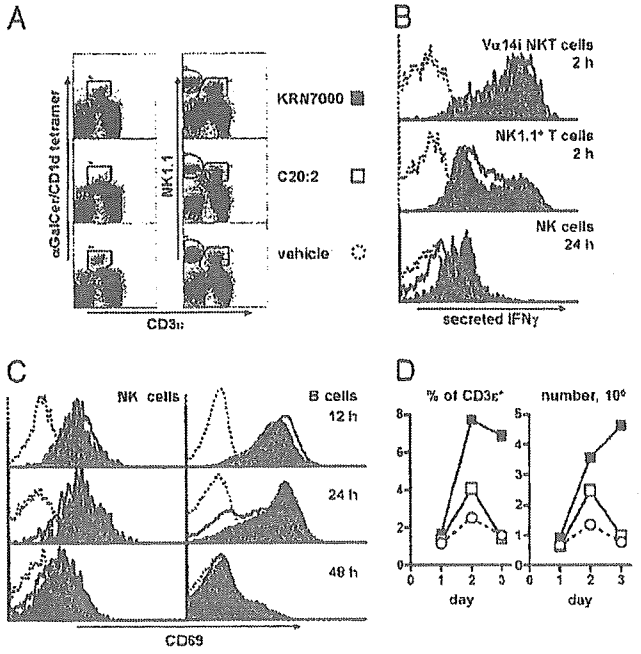

Fig. 4. Sequelae of KRN7000 and C20:2-induced Vα14i NKT cell activation. (*A*) Vα14i NKT cell (tetramer$^+$ CD3ε^{int}), NK cell (NK1.1$^+$ CD3ε^-), and NK1.1$^+$ T cell (NK1.1^{int} CD3ε^{int}) identification by FACS in splenocytes from mice given KRN7000, C20:2, or vehicle i.p. 2 h earlier. Lymphocytes gated as negative for B220 and propidium iodide are shown. (*B*) Histogram profiles for IFN-γ secretion of splenic Vα14i NKT, NK1.1$^+$ T, or NK cells from mice 2 or 24 h after treatment with glycolipid. IFN-γ-staining in C24:0-stimulated samples was identical to that of KRN7000-stimulated samples. (*C*) CD69 levels of splenic NK cells (gated as CD3ε^- NK1.1$^+$) or B cells (CD3ε^- NK1.1$^-$ B220$^+$) at 12, 24, or 48 h after injection of glycolipid. (*D*) Splenic Vα14i NKT cell (B220$^-$ CD3ε^{int} tetramer$^+$) frequency, measured as either percentages of T cells or as total NKT cell number, in mice 1, 2, or 3 days after glycolipid administration. The results shown are representative of three independent experiments.

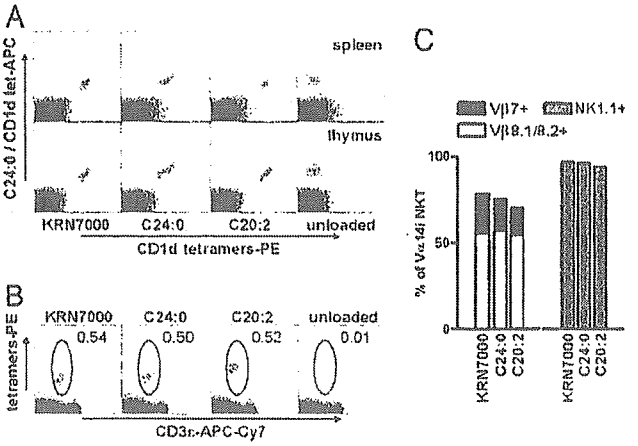

Fig. 5. Recognition of KRN7000, C24:0, and C20:2 by the same population of Vα14i NKT cells. (*A*) Costaining of C57BL/6 splenocytes or thymocytes with allophycocyanin-conjugated CD1d tetramers assembled with C24:0, and phycoerythrin-labeled CD1d tetramers assembled with various analogues. (*B*) Thymocytes were stained with C24:0, C20:2, KRN7000, or vehicle-loaded CD1d tetramers–phycoerythrin, and with antibodies to B220, CD3ε, Vβ7, Vβ8.1/8.2, or NK1.1. Dot plots show gating for tetramer$^+$ T cells, after exclusion of B lymphocytes, and dead cells. (*C*) TCR Vβ and NK1.1 phenotype of tetramer$^+$ CD3ε^{int} thymocytes. Analogous results were obtained with splenocytes. The results shown are representative of three or more experiments.

that cytokine polarization observed after C20:2 administration was not due to differences in the initial Vα14i NKT cell response but, rather, reflected altered downstream events such as the relatively late IFN-γ production by activated NK cells.

Secreted cytokine staining confirmed that in both KRN7000- and C20:2-treated mice, NK cells were IFN-γ$^+$ at 6–12 h after treatment (26, 27). However, whereas splenic NK cells from mice that received either KRN7000 or the closely related C24:0 analogue strongly produced IFN-γ as late as 24 h after initial activation, NK cells from C20:2-treated mice showed substantially reduced staining (Fig. 4*B*). Together, these results pointed to a less sustained secondary IFN-γ production by NK cells (rather than a change in the initial cytokine response of Vα14i NKT cells) as the major factor responsible for the T_H2 bias of the systemic cytokine response to C20:2.

Sequelae of Vα14i NKT Cell Activation by C20:2. Secondary activation of bystander B and NK cells after KRN7000 administration has been studied by using expression of the activation marker CD69 (26, 28–30). We followed CD69 expression of splenic NK and B cell populations for several hours after KRN7000 or C20:2 administration. Both populations began to up-regulate CD69 at 4–6 h after injection (data not shown). Paradoxically, C20:2 induced slightly higher CD69 levels on both cell populations up until 12 h, although this trend was reversed from 24 h onwards, suggesting an earlier up-regulation yet faster subsequent down-regulation of the marker (Fig. 4*C*). NK cell forward scatter likewise remained higher in KRN7000-treated mice at days 1–3 compared with C20:2-treated mice (data not shown).

It is established that Vα14i NKT cells expand beyond homeostatic levels 2 or 3 days after KRN7000 stimulation (24, 25). In our study, a 3- to 5-fold expansion in splenic Vα14i NKT cell number occurred in KRN7000-treated mice at day 3 after injection. Interestingly, after *in vivo* administration of C20:2, only a minimal transient expansion was observed on day 2, with no expansion of the Vα14i NKT cell population thereafter, even as late as day 5 (Fig. 4*D* and data not shown). Together, our findings indicated pronounced alterations in the late sequelae of Vα14i NKT cell activation with the C20:2 analogue compared with KRN7000.

Recognition of KRN7000 and C20:2 by Identical Cell Populations. CD1d complexes containing the α-GalCer analogue OCH have been shown to have significantly reduced avidity for TCRs of Vα14i NKT cells compared with binding of KRN7000-loaded complexes (31). This finding suggests the possibility that the T_H2-biased response of C20:2 could be a result of preferential stimulation of Vα14i NKT cell subsets with TCRs of higher affinity for lipid-loaded CD1d. In fact, phenotypically defined subsets of murine and human NKT cells have been described that show a bias toward increased production of IL-4 relative to IFN-γ upon stimulation (32–36). However, by costaining of splenic and thymic Vα14i NKT cells by using CD1d tetramers loaded with different lipids, we demonstrated that identical populations recognized C24:0, C20:2, and KRN7000 (Fig. 5*A*). Single staining with these reagents revealed no difference in Vβ usage or NK1.1 status of cells reactive with the different analogue tetramers (Fig. 5 *B* and *C*). Interestingly, C20:2-loaded tetramers stained NKT cells more strongly than tetramers loaded with KRN7000, reflecting a slightly higher affinity of the C20:2–CD1d complex to the Vα14i TCR (J.S.I. and S.A.P., unpublished results). Together, these findings demonstrated that the altered cytokine response to C20:2 cannot be the result of preferential activation of a subset of Vα14i NKT cells.

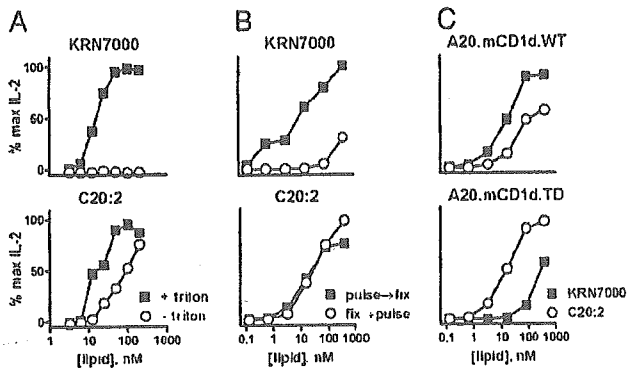

Fig. 6. Differential requirements for CD1d loading with KRN7000 and C20:2. IL-2 response of hybridoma DN3A4–1.2 to glycolipid presentation in three *in vitro* CD1d presentation systems: platebound CD1d loaded with varying amounts of KRN7000 or C20:2 in the presence or absence of the detergent Triton X-100 (*A*), RMA-S.CD1d cells pulsed with glycolipid before or after glutaraldehyde fixation (*B*), or WT or cytoplasmic tail-deleted (TD) CD1d-transfected A20 cells, loaded with either KRN7000 or C20:2 (*C*).

Loading Requirements of α-GalCer Analogues onto CD1d. To find an alternative explanation for the T_H2-biased response to C20:2, we studied requirements for handling of different forms of α-GalCer by antigen-presenting cells. We employed a cell-free system in which platebound mouse CD1d was loaded with doses of KRN7000 or C20:2 in the presence or absence of the detergent Triton X-100 (37). By using IL-2 production by DN3A4–1.2 as a readout for glycolipid loading of CD1d, we observed a marked dependence on detergent for loading of KRN7000 but not for C20:2 (Fig. 6*A*). This result suggested a significant difference in requirement for cofactors, such as acidic pH or lipid transfer proteins, that facilitate lipid loading onto CD1d in endosomes (38–41). We assessed this hypothesis further by using glutaraldehyde fixation of $CD1d^+$ antigen-presenting cells, which blocks antigen uptake and recycling of CD1d between endosomes and the plasma membrane. Vα14i NKT cell recognition of KRN7000 was markedly reduced if lipid loading was done after fixation of RMA-S.mCD1d cells, whereas recognition of C20:2 was unimpaired (Fig. 6*B*).

Similar conclusions were drawn from experiments by using A20 cells transfected with either WT or cytoplasmic tail-deleted CD1d (Fig. 6*C*). The tail-deleted CD1d mutant lacks the intracellular tyrosine-based sorting motif required for internalization and endosomal localization of CD1d (19). As was the case with RMA-S.mCD1d, WT CD1d-transfected A20 cells presented KRN7000 more potently than C20:2. However, the tail-deleted mutant presented C20:2 with at least 20-fold greater efficiency than KRN7000. Together, these results point to the conclusion that the T_H2-skewing C20:2 analogue had substantially less dependence on endosomal loading for presentation by CD1d when compared with compounds that produced a more mixed response with strong IFN-γ production, such as KRN7000.

Discussion

This study details *in vitro* and *in vivo* consequences of activation of Vα14i NKT cells with C20:2, a diunsaturated *N*-acyl substituted analogue of the prototypical α-GalCer, KRN7000. The T_H2 cytokine bias observed with C20:2 is not unique: OCH and other shortened fully saturated lipids have been shown to have this effect (13, 42). C20:2 differs from these other compounds in two potentially important respects. First, the *in vitro* potency of C20:2 for stimulation of certain Vα14i NKT cell functions (e.g., proliferation and secretion of IL-4 and IL-2) approaches that of KRN7000, whereas OCH appears to be a much weaker Vα14i NKT cell agonist. Second, staining with C20:2-loaded CD1d tetramers, as opposed to OCH, is undiminished compared with KRN7000. This finding would suggest that, as a therapeutic agent, C20:2 will be recognized by the identical global Vα14i NKT cell population (as KRN7000 is) and not limited to higher-affinity NKT cell subsets, as suggested for OCH (31).

A recent study showed that one mechanism by which OCH may induce a T_H2-biased cytokine response involves changes in IFN-γ production by Vα14i NKT cells themselves. Oki *et al.* (43) reported that the transcription factor gene *c-Rel*, a member of the NF-κB family of transcriptional regulators that is a crucial component of IFN-γ production, is inducibly transcribed in KRN7000-stimulated but not OCH-stimulated Vα14i NKT cells. Although we have not assessed *c-Rel* induction or other factors involved in IFN-γ production in response to C20:2, our findings did not suggest that early IFN-γ production by Vα14i NKT cells was different after activation with C20:2 versus KRN7000. Both lipids induced identical single-cell IFN-γ staining in Vα14i NKT cells and serum IFN-γ levels at 2 h after injection. However, in contrast to the apparent similarity in Vα14i NKT cells, NK cell IFN-γ production was significantly reduced and less sustained after *in vivo* administration of C20:2 compared with KRN7000. Hence, failure of C20:2 to fully activate downstream events leading to optimal NK cell secondary stimulation by activated Vα14i NKT cells appears to be the most likely mechanism by which C20:2 induces reduced IFN-γ and an apparent T_H2-biased systemic response.

C20:2 administration resulted also in a more rapid but less sustained CD69 up-regulation in NK and B cells, as well as a lack of a substantial Vα14i NKT cell expansion. These findings were surprising, given that TCR down-modulation observed on Vα14i NKT cells within the first few hours after C20:2 stimulation was similar to or greater than that induced by KRN7000 (Fig. 4*A* and data not shown), indicating strong TCR signaling in response to the analogue. These features of the response to C20:2 may be a further reflection of the failure of C20:2 to induce a full range of downstream events after Vα14i NKT cell activation, including the production of cytokines or other factors required to support the expansion of Vα14i NKT cells.

What mechanism can then be invoked to account for the altered cytokine response to C20:2 and other *N*-acyl variants of KRN7000? One intriguing possibility is provided by our analysis of requirements for presentation of C20:2 compared with KRN7000, which revealed marked differences between these glycolipids in their need for endosomal loading onto CD1d. CD1d and other CD1 proteins undergo transport into the endocytic pathway, leading to intracellular loading with lipid antigens and subsequent recycling to the cell surface (39). The importance of endosomal loading for KRN7000 most likely reflects the impact of factors in these compartments that facilitate the insertion of lipids into the CD1d ligand-binding groove. These factors include the acidic pH of the endosomal environment, as well as lipid transport proteins, such as saposins and GM2 activator protein (38, 40, 41). Our findings indicate that C20:2 can efficiently load onto CD1d in the absence of these endosomal cofactors. Consequently, we speculate that C20:2 may be strongly presented by any cell type that expresses surface CD1d, regardless of its ability to efficiently endocytose lipids from the extracellular space. This more widespread presentation could lead to a more pronounced presentation of C20:2 by nonprofessional antigen-presenting cell types compared with KRN7000. Because many cell types express CD1d, including all hematopoietic lineages and various types of epithelia (44–48), presentation of C20:2 by nonprofessional antigen-presenting cells may explain the more rapid trans-activation of bystander cells observed with C20:2. An alternative hypothesis is that the endosomal loading requirements of KRN7000 result in its preferential localization into CD1d molecules contained in membrane lipid rafts, whereas the permissive loading properties of

C20:2 would result in a more uniform glycolipid distribution across the cell membrane. Evidence of lipid raft localization of CD1d and raft influence on the T_H-bias of MHC class II-restricted $CD4^+$ T cells lend support to this model (49, 50). Either scenario would be expected to result in decreased delivery of costimulatory signals associated with professional antigen-presenting cells (e.g., dendritic cells) and, thus, lead to quantitative and qualitative differences in the outcome of Vα14i NKT cell stimulation. Consistent with both models, Vα14i NKT cell activation with KRN7000 *in vitro* in the presence of costimulatory blockade (anti-CD86) can polarize cytokine production to a T_H2 profile (22).

We have shown that structurally modified forms of α-GalCer with alterations in their *N*-acyl substituents can be designed to generate potent immunomodulators that stimulate qualitatively altered responses from Vα14i NKT cells. Our results confirm and extend several basic observations and principles established from earlier studies on less potent agonists, such as OCH. Further study of these and similar analogues may yield compounds with clear advantages for treatment or prevention of specific immunologic disorders or for the stimulation of protective host immunity against particular pathogens.

We thank R. Koganty and S. Gandhi (Biomira) for sharing their panel of synthetic glycosylceramides, which included compound BF1508-84; M. Kronenberg for the recombinant baculovirus used for production of soluble mouse CD1d; M. Taniguchi, T. Nakayama, A. Bendelac, M. Exley, S. Balk, S. Behar, and M. Kronenberg for gifts of mice and cell lines; Z. Hu for expert technical assistance; and T. DiLorenzo for critical reading of this manuscript. This work was supported by National Institutes of Health Grants A145889, A148933, and DK068690 (to S.A.P.), the Japan Human Sciences Foundation (T.Y. and S.A.P.), the Pharmaceutical and Medical Devices Agency (T.Y.), Medical Research Council Grants G9901077 and G0000895 (to G.S.B.), and Wellcome Trust Grants 060750 and 072021 (to G.S.B.). G.S.B. is a Lister Jenner Research Fellow.

1. Lantz, O. & Bendelac, A. (1994) *J. Exp. Med.* **180,** 1097–1106.
2. Brossay, L. & Kronenberg, M. (1999) *Immunogenetics* **50,** 146–151.
3. Godfrey, D. I., Hammond, K. J., Poulton, L. D., Smyth, M. J. & Baxter, A. G. (2000) *Immunol. Today* **21,** 573–583.
4. Wilson, S. B. & Delovitch, T. L. (2003) *Nat. Rev. Immunol.* **3,** 211–222.
5. Poulton, L. D., Smyth, M. J., Hawke, C. G., Silveira, P., Shepherd, D., Naidenko, O. V., Godfrey, D. I. & Baxter, A. G. (2001) *Int. Immunol.* **13,** 887–896.
6. Gombert, J.-M., Tancrede-Bohin, T., Hameg, A., do Carmo Leite-de-Moraes, M., Vicari, A. P., Bach, J.-F. & Herbelin, A. (1996) *Int. Immunol.* **8,** 1751–1758.
7. Van Der Vliet, H. J., Von Blomberg, B. M., Nishi, N., Reijm, M., Voskuyl, A. E., van Bodegraven, A. A., Polman, C. H., Rustemeyer, T., Lips, P., Van Den Eertwegh, A. J., *et al.* (2001) *Clin. Immunol.* **100,** 144–148.
8. Taniguchi, M., Harada, M., Kojo, S., Nakayama, T. & Wakao, H. (2003) *Annu. Rev. Immunol.* **21,** 483–513.
9. Kawano, T., Cui, J., Koezuka, Y., Toura, I., Kaneko, Y., Motoki, K., Ueno, H., Nakagawa, R., Sato, H., Kondo, E., *et al.* (1997) *Science* **278,** 1626–1629.
10. Wang, B., Geng, Y. B. & Wang, C. R. (2001) *J. Exp. Med.* **194,** 313–320.
11. Sharif, S., Arreaza, G. A., Zucker, P., Mi, Q. S., Sondhi, J., Naidenko, O. V., Kronenberg, M., Koezuka, Y., Delovitch, T. L., Gombert, J. M., *et al.* (2001) *Nat. Med.* **7,** 1057–1062.
12. Hong, S., Wilson, M. T., Serizawa, I., Wu, L., Singh, N., Naidenko, O. V., Miura, T., Haba, T., Scherer, D. C., Wei, J., *et al.* (2001) *Nat. Med.* **7,** 1052–1056.
13. Miyamoto, K., Miyake, S. & Yamamura, T. (2001) *Nature* **413,** 531–534.
14. Mizuno, M., Masumura, M., Tomi, C., Chiba, A., Oki, S., Yamamura, T. & Miyake, S. (2004) *J. Autoimmun.* **23,** 293–300.
15. Sonoda, K. H., Exley, M., Snapper, S., Balk, S. P. & Stein-Streilein, J. (1999) *J. Exp. Med.* **190,** 1215–1226.
16. Cui, J., Shin, T., Kawano, T., Sato, H., Kondo, E., Toura, I., Kaneko, Y., Koseki, H., Kanno, M. & Taniguchi, M. (1997) *Science* **278,** 1623–1626.
17. Behar, S. M., Podrebarac, T. A., Roy, C. J., Wang, C. R. & Brenner, M. B. (1999) *J. Immunol.* **162,** 161–167.
18. Brossay, L., Tangri, S., Bix, M., Cardell, S., Locksley, R. & Kronenberg, M. (1998) *J. Immunol.* **160,** 3681–3688.
19. Prigozy, T. I., Naidenko, O., Qasba, P., Elewaut, D., Brossay, L., Khurana, A., Natori, T., Koezuka, Y., Kulkarni, A. & Kronenberg, M. (2001) *Science* **291,** 664–667.
20. Porcelli, S., Morita, C. T. & Brenner, M. B. (1992) *Nature* **360,** 593–597.
21. Matsuda, J. L., Naidenko, O. V., Gapin, L., Nakayama, T., Taniguchi, M., Wang, C. R., Koezuka, Y. & Kronenberg, M. (2000) *J. Exp. Med.* **192,** 741–754.
22. Pal, E., Tabira, T., Kawano, T., Taniguchi, M., Miyake, S. & Yamamura, T. (2001) *J. Immunol.* **166,** 662–668.
23. Matsuda, J. L., Gapin, L., Baron, J. L., Sidobre, S., Stetson, D. B., Mohrs, M., Locksley, R. M. & Kronenberg, M. (2003) *Proc. Natl. Acad. Sci. USA* **100,** 8395–8400.
24. Crowe, N. Y., Uldrich, A. P., Kyparissoudis, K., Hammond, K. J., Hayakawa, Y., Sidobre, S., Keating, R., Kronenberg, M., Smyth, M. J. & Godfrey, D. I. (2003) *J. Immunol.* **171,** 4020–4027.
25. Wilson, M. T., Johansson, C., Olivares-Villagomez, D., Singh, A. K., Stanic, A. K., Wang, C. R., Joyce, S., Wick, M. J. & Van Kaer, L. (2003) *Proc. Natl. Acad. Sci. USA* **100,** 10913–10918.
26. Carnaud, C., Lee, D., Donnars, O., Park, S. H., Beavis, A., Koezuka, Y. & Bendelac, A. (1999) *J. Immunol.* **163,** 4647–4650.
27. Schmieg, J., Yang, G., Franck, R. W. & Tsuji, M. (2003) *J. Exp. Med.* **198,** 1631–1641.
28. Hayakawa, Y., Takeda, K., Yagita, H., Kakuta, S., Iwakura, Y., Van Kaer, L., Saiki, I. & Okumura, K. (2001) *Eur. J. Immunol.* **31,** 1720–1727.
29. Eberl, G. & MacDonald, H. R. (2000) *Eur. J. Immunol.* **30,** 985–992.
30. Kitamura, H., Ohta, A., Sekimoto, M., Sato, M., Iwakabe, K., Nakui, M., Yahata, T., Meng, H., Koda, T., Nishimura, S., *et al.* (2000) *Cell. Immunol.* **199,** 37–42.
31. Stanic, A. K., Shashidharamurthy, R., Bezbradica, J. S., Matsuki, N., Yoshimura, Y., Miyake, S., Choi, E. Y., Schell, T. D., Van Kaer, L., Tevethia, S. S., *et al.* (2003) *J. Immunol.* **171,** 4539–4551.
32. Benlagha, K., Kyin, T., Beavis, A., Teyton, L. & Bendelac, A. (2002) *Science* **296,** 553–555.
33. Gumperz, J. E., Miyake, S., Yamamura, T. & Brenner, M. B. (2002) *J. Exp. Med.* **195,** 625–636.
34. Lee, P. T., Benlagha, K., Teyton, L. & Bendelac, A. (2002) *J. Exp. Med.* **195,** 637–641.
35. Gadue, P. & Stein, P. L. (2002) *J. Immunol.* **169,** 2397–2406.
36. Pellicci, D. G., Hammond, K. J., Uldrich, A. P., Baxter, A. G., Smyth, M. J. & Godfrey, D. I. (2002) *J. Exp. Med.* **195,** 835–844.
37. Sidobre, S., Naidenko, O. V., Sim, B. C., Gascoigne, N. R., Garcia, K. C. & Kronenberg, M. (2002) *J. Immunol.* **169,** 1340–1348.
38. Kang, S. J. & Cresswell, P. (2004) *Nat. Immunol.* **5,** 175–181.
39. Moody, D. B. & Porcelli, S. A. (2003) *Nat. Rev. Immunol.* **3,** 11–22.
40. Winau, F., Schwierzeck, V., Hurwitz, R., Remmel, N., Sieling, P. A., Modlin, R. L., Porcelli, S. A., Brinkmann, V., Sugita, M., Sandhoff, K., *et al.* (2004) *Nat. Immunol.* **5,** 169–174.
41. Zhou, D., Cantu, C., III, Sagiv, Y., Schrantz, N., Kulkarni, A. B., Qi, X., Mahuran, D. J., Morales, C. R., Grabowski, G. A., Benlagha, K., *et al.* (2004) *Science* **303,** 523–527.
42. Goff, R. D., Gao, Y., Mattner, J., Zhou, D., Yin, N., Cantu, C., III, Teyton, L., Bendelac, A. & Savage, P. B. (2004) *J. Am. Chem. Soc.* **126,** 13602–13603.
43. Oki, S., Chiba, A., Yamamura, T. & Miyake, S. (2004) *J. Clin. Invest.* **113,** 1631–1640.
44. Bonish, B., Jullien, D., Dutronc, Y., Huang, B. B., Modlin, R., Spada, F. M., Porcelli, S. A. & Nickoloff, B. J. (2000) *J. Immunol.* **165,** 4076–4085.
45. Colgan, S. P., Pitman, R. S., Nagaishi, T., Mizoguchi, A., Mizoguchi, E., Mayer, L. F., Shao, L., Sartor, R. B., Subjeck, J. R. & Blumberg, R. S. (2003) *J. Clin. Invest.* **112,** 745–754.
46. Brossay, L., Jullien, D., Cardell, S., Sydora, B. C., Burdin, N., Modlin, R. L. & Kronenberg, M. (1997) *J. Immunol.* **159,** 1216–1224.
47. Park, S. H., Roark, J. H. & Bendelac, A. (1998) *J. Immunol.* **160,** 3128–3134.
48. Roark, J. H., Park, S. H., Jayawardena, J., Kavita, U., Shannon, M. & Bendelac, A. (1998) *J. Immunol.* **160,** 3121–3127.
49. Lang, G. A., Maltsev, S. D., Besra, G. S. & Lang, M. L. (2004) *Immunology* **112,** 386–396.
50. Boutois, V., Baillet, M., Becart, S., Mooney, N., Leserman, L. & Machy, P. (2003) *J. Immunol.* **171,** 5812–5819.

IFN-γ–mediated negative feedback regulation of NKT-cell function by CD94/NKG2

Tsuyoshi Ota, Kazuyoshi Takeda, Hisaya Akiba, Yoshihiro Hayakawa, Kouetsu Ogasawara, Yoshinori Ikarashi, Sachiko Miyake, Hiro Wakasugi, Takashi Yamamura, Mitchell Kronenberg, David H. Raulet, Katsuyuki Kinoshita, Hideo Yagita, Mark J. Smyth, and Ko Okumura

Activation of invariant natural killer T (iNKT) cells with CD1d-restricted T-cell receptor (TCR) ligands is a powerful means to modulate various immune responses. However, the iNKT-cell response is of limited duration and iNKT cells appear refractory to secondary stimulation. Here we show that the CD94/NKG2A inhibitory receptor plays a critical role in down-regulating iNKT-cell responses. Both TCR and NK-cell receptors expressed by iNKT cells were rapidly down-modulated by priming with α-galactosylceramide (α-GalCer) or its analog OCH [(2*S*,3*S*,4*R*)-1-*O*-(α-D-galactopyranosyl)-*N*-tetracosanoyl-2-amino-1,3,4-nonanetriol)]. TCR and CD28 were re-expressed more rapidly than the inhibitory NK-cell receptors CD94/NKG2A and Ly49, temporally rendering the primed iNKT cells hyperreactive to ligand restimulation. Of interest, α-GalCer was inferior to OCH in priming iNKT cells for subsequent restimulation because α-GalCer–induced interferon γ (IFN-γ) up-regulated Qa-1^b expression and Qa-1^b in turn inhibited iNKT-cell activity via its interaction with the inhibitory CD94/NKG2A receptor. Blockade of the CD94/NKG2–Qa-1^b interaction markedly augmented recall and primary responses of iNKT cells. This is the first report to show the critical role for NK-cell receptors in controlling iNKT-cell responses and provides a novel strategy to augment the therapeutic effect of iNKT cells by priming with OCH or blocking of the CD94/NKG2A inhibitory pathway in clinical applications. (Blood. 2005;106:184-192)

Introduction

Natural killer T (NKT) cells are a special T-cell population coexpressing the T-cell receptor (TCR) and NK-cell receptors such as NK1.1.[1-4] Invariant NKT (iNKT) cells express a Vα14Jα18 chain (Vα24Jα15 in humans) and a semivariant TCR β-chain that is largely biased toward Vβ8.2 (Vβ11 in humans), Vβ2, and Vβ7.[1-4] This TCR recognizes glycolipid antigens, such as α-galactosylceramide (α-GalCer), its analogs including OCH (a sphingosine-truncated analog of α-GalCer; (2*S*,3*S*,4*R*)-1-*O*-(α-D-galactopyranosyl)-*N*-tetracosanoyl-2-amino-1,3,4-nonanetriol), and isoglobotrihexosylceramide (iGb3), presented on the major histocompatibility complex (MHC) class I–like molecule CD1d.[1-10] In addition, costimulatory signals, mediated through antigen-presenting cells that express CD80/86 interacting with CD28 expressed by iNKT cells, critically regulate iNKT-cell activation in a similar manner to conventional T cells.[11,12] One of most striking characteristics of iNKT cells is their ability to promptly secrete various cytokines, including both interferon γ (IFN-γ) and interleukin 4 (IL-4), after their encounter with antigens (Ag's),[1-4] which is reminiscent of effector/memory T cells. Accordingly, iNKT cells are thought to be potent immunoregulatory cells and their activation by ligands, such as α-GalCer and OCH, has been shown to be a powerful means to modulate various immune responses, including protective immunity, autoimmunity, and antitumor immunity.[1-4,6,9,11,13,14]

Despite an accumulation of studies concerning iNKT-cell activation of bystander immune cells, relatively little is known about the fate of Ag-primed iNKT cells themselves. Previous studies have shown that iNKT cells disappear quickly after their activation following TCR ligation or IL-12 stimulation.[15-17] This phenomenon was initially attributed to increased activation-induced cell death (AICD) of iNKT cells, consistent with repopulation and homeostatic proliferation of peripheral iNKT cells after their rapid recruitment from the bone marrow.[15] More recently, however, several studies have reported that down-regulation of TCR and NK1.1 cell surface expression on iNKT cells is the primary reason for the apparent disappearance of iNKT cells following α-GalCer treatment.[18-20] Indeed a substantial iNKT-cell proliferation was observed in peripheral lymphoid organs following

From the Departments of Immunology, and Obstetrics and Gynecology, Juntendo University School of Medicine, Tokyo, Japan; Cancer Immunology Program, Sir Donald and Lady Trescowthick Laboratories, Peter MacCallum Cancer Centre, Melbourne, Victoria, Australia; Department of Microbiology and Immunology and the Cancer Research Institute, University of California San Francisco, San Francisco, CA; Pharmacology Division, National Cancer Center Research Institute, Tokyo, Japan; Department of Immunology, National Institute of Neuroscience, National Center of Neurology and Psychiatry, Kodaira, Tokyo, Japan; Division of Developmental Immunology, La Jolla Institute for Allergy and Immunology, San Diego, CA; and Department of Molecular and Cell Biology and Cancer Research Laboratory, University of California, Berkeley, CA.

Submitted November 8, 2004; accepted February 27, 2005. Prepublished online as *Blood* First Edition Paper, March 3, 2005; DOI 10.1182/blood-2004-11-4257.

Supported by research grants from the Human Frontier Science Program Organization; the Organization for Pharmaceutical Safety and Research; the Ministry of Education, Science, and Culture, Japan; the National Health and Medical Research Council of Australia; and the National Institutes of Health.

T.O. and K.T. contributed equally to this work.

Reprints: Kazuyoshi Takeda, Department of Immunology, Juntendo University School of Medicine, 2-1-1 Hongo, Bunkyo-ku, Tokyo 113-8421, Japan; e-mail: ktakeda@med.juntendo.ac.jp.

The publication costs of this article were defrayed in part by page charge payment. Therefore, and solely to indicate this fact, this article is hereby marked "advertisement" in accordance with 18 U.S.C. section 1734.

α-GalCer treatment.[18-20] These findings suggested an interesting possibility that Ag-primed iNKT cells may develop an effector/memory subpopulation, which exerts even more potent function than unprimed iNKT cells. Here, we now demonstrate that priming of iNKT cells with their TCR ligands induces a dynamic modulation of TCR, NK-cell receptors (NK1.1, CD94/NKG2, NKG2D, and Ly49), and a costimulatory receptor (CD28). Differential kinetics of re-expression of these molecules on the cell surface temporally renders the primed iNKT cells hyperresponsive to secondary Ag stimulation. Of importance, the recall response of α-GalCer–primed iNKT cells is strictly regulated by an IFN-γ–dependent negative feedback mechanism where IFN-γ upregulates Qa-1^b expression and subsequent ligation of CD94/NKG2 inhibits iNKT-cell activity. Although Qa-1^b can interact with NKG2A, NKG2C, and NKG2E, it has been previously reported that the majority of CD94/NKG2 expressed in mice is the inhibitory CD94/NKG2A receptor and that the Qa-1^b–CD94/NKG2A interaction plays a critical role in negative regulation of NK-cell responses to self.[21-23] We confirm that iNKT cells preferentially express CD94/NKG2A and hence blockade of the Qa-1^b–NKG2A interaction markedly augmented recall responses of primed iNKT cells and primary responses of naive iNKT cells to α-GalCer. These findings are an important step to improve the efficacy of iNKT-cell–targeting therapeutics against tumor, infection, and autoimmune diseases since they demonstrate a means to modulate the adjuvant nature of iNKT cells by combined treatment with iNKT-cell glycolipid ligands and antagonistic monoclonal antibodies (mAbs).

Materials and methods

Mice

Wild-type (WT) C57BL/6 (B6) mice were obtained from Charles River Japan (Yokohama, Japan). IFN-γ–deficient (IFN-$\gamma^{-/-}$) B6 mice were kindly provided by Y. Iwakura (University of Tokyo).[24] All mice were maintained under specific pathogen-free conditions and used in accordance with the institutional guidelines of Juntendo University.

Reagents

A synthetic form of α-GalCer was obtained from Kirin Brewery (Gunma, Japan) and OCH was derived as described previously.[6] In most experiments, mice were intraperitoneally injected with 2 μg of α-GalCer or OCH in 200 μL of phosphate-buffered saline (PBS) for priming and boosting. Dimethyl sulfoxide (DMSO; 0.1%) was used as the vehicle control. Phycoerythrin (PE)-conjugated tetrameric CD1d molecules loaded with α-GalCer (α-GalCer/CD1d) were prepared as described.[17] The anti-NKG2A/C/E (NKG2) mAb, 20d5, and the anti-NKG2D mAb (CX5) were generated as described previously.[21,25] Fab fragments of 20d5 and anti–Qa-1^b mAb (BD Pharmingen, San Diego, CA) were prepared using the Fab preparation kit (Pierce, Rockford, IL) as described.[26]

Flow cytometric analysis

Mononuclear cells (MNCs) were prepared from spleen and liver as described.[11] Cells were first preincubated with antimouse CD16/32 (2.4G2) mAb to avoid nonspecific binding of mAbs to FcγR. Surface and intracellular expression of molecules by iNKT cells were analyzed on electronically gated α-GalCer/CD1d tetramer$^+$ cells on 4-color flow cytometry using a FACSCaliber (BD Bioscience, San Jose, CA). Intracellular staining was performed with a BD Cytofix/Cytoperm kit (BD Pharmingen) according to the manufacturer's instructions. Intracellular TCR in NKT cells was detected with a mixture of PE-conjugated antimouse Vβ2 TCR mAb (B20.6), anti-Vβ7 TCR mAb (TR310), and anti-Vβ8 TCR mAb (F23.1), or α-GalCer–loaded recombinant soluble dimeric mouse CD1d: immunoglobulin (CD1d:Ig; BD Pharmingen) and PE-conjugated anti–mouse IgG1 mAb (A85-1; BD Pharmingen). Surface and intracellular molecules were analyzed on electronically gated intracellular Vβ2/7/8$^+$ cells 1 day after α-GalCer or OCH injection. Surface and intracellular molecules were stained with fluorescein isothiocyanate (FITC)– or allophycocyanin (APC)–conjugated NK1.1 mAb (PK136); FITC- or biotin-conjugated antimouse CD94 mAb (18d3); FITC- or biotin-conjugated antimouse NKG2A/C/E (NKG2) mAb (20d5); biotin-conjugated antimouse NKG2A^{B6} (16a11); FITC-conjugated antimouse Ly49 mAbs (anti-Ly49D mAb [4E5] or a mixture of anti-Ly49A^{B6} [A1], anti-Ly49C/I mAb [5E6], anti-Ly49G2 mAb [4D11], and antimouse Ly49I mAb [YL1-90]); biotin-conjugated anti-NKG2D mAb (CX5); APC- or biotin-conjugated anti-mouse CD28 mAb (37.51); biotin-conjugated antimouse Qa-1^b mAb (6A8.6F10.1A6); FITC-, PE-, PE–cyanin 5 (PE-Cy5)–, APC-, or biotin-conjugated isotype-matched control mAbs (G155-178, MOPC-31C, R35-95, A95-1, R3-34, and Ha4/8); and Cy5-conjugated streptavidin. All of these reagents were purchased from BD Pharmingen, except for antimouse CD94 mAb, anti-NKG2A^{B6} mAb, anti-NKG2D mAb, and anti-CD28 mAb from eBioscience (San Diego, CA).

Cell preparation and in vitro stimulation

Freshly isolated splenic MNCs from vehicle-, α-GalCer–, or OCH-primed mice (5×10^5) were cultured in RPMI 1640 medium supplemented with 10% heat-inactivated fetal calf serum (FCS), 2 mM L-glutamine, and 25 mM $NaHCO_3$ in humidified 5% CO_2 at 37°C in 96-well U-bottom plates (Corning, Corning, NY) as previously described.[11] Cells were stimulated with 100 ng/mL α-GalCer, OCH, or vehicle (0.1% DMSO) in the presence or absence of 10-μg/mL Fab fragments of isotype-matched control mAbs, anti-NKG2 mAb, or antimouse Qa-1^b mAb, or intact antimouse CD80 (16-10A1) and antimouse CD86 (PO 3.1) mAbs (eBioscience). After 24 to 48 hours, cell-free culture supernatants were harvested to determine IFN-γ and IL-4 levels by enzyme-linked immunosorbent assay (ELISA).

Coculture of iNKT cells and DCs

Freshly isolated hepatic MNCs were stained with PE-conjugated α-GalCer/CD1d tetramer, and positive cells were enriched by autoMACS using anti-PE microbeads (Miltenyi Biotec, Bergisch Gladbach, Germany) according to the manufacturer's instructions. Enriched iNKT cells were then sorted on a FACS Vantage (BD Bioscience) to obtain highly purified (98%-99%) iNKT cells. Splenic dendritic cells (DCs) were prepared according to the reported method.[27,28] Purified iNKT cells (10^5) and DCs (5×10^4) were cocultured as previously described[11,29,30] with 100 ng/mL α-GalCer or vehicle (0.1% DMSO) in the presence or absence of 10-μg/mL Fab fragments of isotype-matched control mAbs, anti-NKG2A mAb, or anti–Qa-1^b mAb. After 24 to 72 hours, cell-free culture supernatants were harvested to determine IFN-γ and IL-4 levels by ELISA.

ELISA

IFN-γ and IL-4 levels in the culture supernatants or the sera were determined by using mouse IFN-γ– or IL-4–specific ELISA kits (OptEIA; BD Bioscience Pharmingen) according to the manufacturer's instructions.

Cytotoxicity assay

Cytotoxic activity was tested against NK-cell–sensitive YAC-1 cells and NK-cell–resistant P815 cells by a standard 4-hour ^{51}Cr-release assay as previously described.[11] Effector cells (hepatic and splenic MNCs) were prepared from mice 24 hours after the last intraperitoneal injection of α-GalCer, OCH, or vehicle. Some mice were administered with 300 μg of isotype-matched control Ig or anti-NKG2 mAb intraperitoneally 2 days before the last α-GalCer injection. Specific cytotoxicity was calculated as previously described.[11]

Experimental lung metastases

B6 mice were intraperitoneally injected with OCH, α-GalCer, or vehicle, and then intravenously inoculated with B16 melanoma cells (1×10^5,

3×10^5, or 5×10^5/200 μL) 2 hours later on day 0. B16 melanoma cells were prepared as previously described.[11,16] Some mice were primed 2.5 days earlier with OCH or α-GalCer. Some mice were administered with 300 μg of isotype-matched control Ig or anti-NKG2 mAb intraperitoneally 2 days before the last α-GalCer injection. On day 14, the number of tumor colonies on the lungs was counted under a dissecting microscope (Olympus, Tokyo, Japan).

Statistical analysis

Data were analyzed by a 2-tailed Student *t* test. *P* values less than .05 were considered significant.

Results

Modulation of costimulatory and NK-cell receptors on iNKT cells upon priming with TCR ligands

We analyzed the modulation of TCR, inhibitory NK-cell receptors (CD94/NKG2 and Ly49A/C/I/G2), activating NK-cell receptors (NK1.1, NKG2D, and Ly49D), and a costimulatory receptor (CD28) on iNKT cells after in vivo priming with synthetic TCR ligands, α-GalCer or OCH. Amongst liver iNKT cells from B6 WT mice, approximately 50% expressed CD94/NKG2 and NKG2D, less than 10% expressed Ly49A/C/I/G2, less than 2% expressed Ly49D, and all constitutively expressed CD28 (Figure 1A). Staining with an NKG2A-specific mAb showed that CD94/NKG2 expressed on iNKT cells was mainly composed of NKG2A (data not shown) but not NKG2C or NKG2E, as previously reported.[22] Upon priming with α-GalCer or OCH, α-GalCer/CD1d tetramer$^+$ iNKT cells seemingly began to disappear within 6 hours (data not shown) and almost completely disappeared at 16 to 24 hours, as previously reported.[15-20] Consistent with recent reports,[18-20] intracellular staining with anti-Vβ2/7/8 mAbs, detecting the predominant TCR β-chains expressed by iNKT cells, clearly showed the presence of liver iNKT cells expressing intracellular TCR at 24 hours after α-GalCer or OCH priming. NK-cell receptors and CD28 were also internalized, although some retention of cell surface CD28 was still detected (Figure 1A). Although staining intensity was relatively weak, intracellular staining with α-GalCer–loaded recombinant soluble dimeric mouse CD1d:Ig also demonstrated the internalized α-GalCer/CD1d–specific TCR coexpressed with intracellular NK1.1 one day after α-GalCer (Figure 1B) or OCH injection (data not shown). Similar results were obtained with spleen MNCs after in vivo priming and with liver MNCs after in vitro priming (data not shown).

After 2 to 3 days, the primed iNKT cells re-expressed TCR and CD28 on their surface. By contrast, a reduced level of surface NK-cell receptors (NK1.1, CD94/NKG2, Ly49, and NKG2D) was maintained for at least 3 to 4 days. After 5 to 7 days, some iNKT cells still expressed a low level of surface NK1.1, but another iNKT-cell population expressed relatively higher levels of NK1.1 compared with naive iNKT cells. After activation, the proportions of CD94/NKG2-, Ly49-, or NKG2D-expressing iNKT cells increased, and the expression levels of CD94/NKG2 and Ly49 were relatively higher than those found on naive iNKT cells. Again, CD94/NKG2 on these iNKT cells was mainly composed of NKG2A as estimated by staining with NKG2A-specific mAb. Consistent with previous reports,[7,9,18-20] TCR ligand priming induced iNKT-cell expansion, although the expansion level was reduced following OCH priming (1.5-3 fold) compared with α-GalCer priming (5-8 fold) (data not shown). Similar results were obtained with spleen MNCs after in vivo priming and with liver MNCs after in vitro priming (data not shown).

Consistent with a previous report that OCH selectively induced T-helper 2 (Th2) cytokine production by iNKT cells,[6] a minor but significant serum IL-4 elevation was observed 3 to 5 hours after priming with OCH, but serum IFN-γ was not detected (Figure 2A). Moreover, we observed a similar modulation of iNKT-cell surface

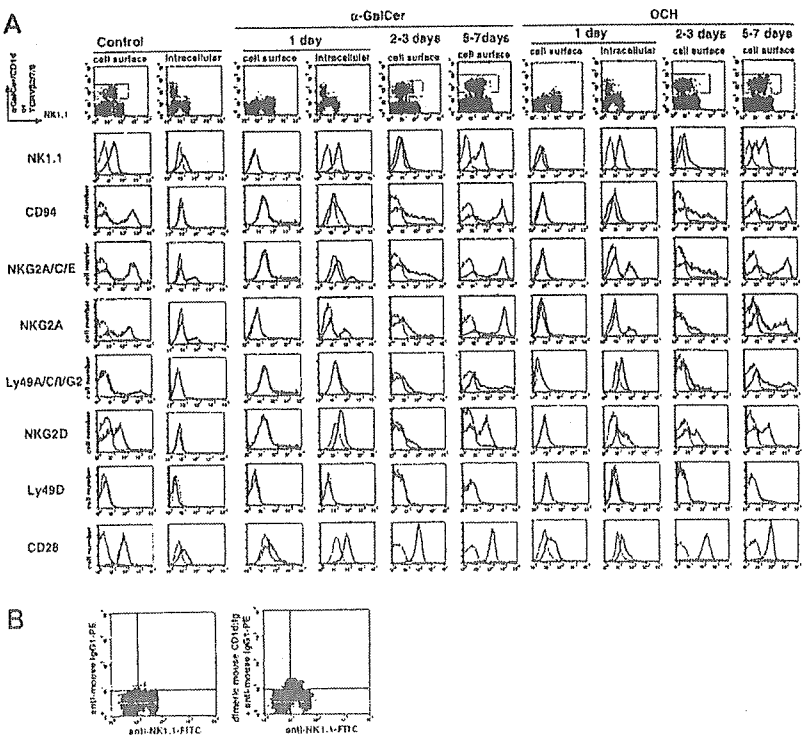

Figure 1. Modulation of NK1.1, CD94/NKG2, Ly49, NKG2D, and CD28 on α-GalCer– or OCH-activated liver iNKT cells. (A) Cell surface expression of the indicated molecules was analyzed on electronically gated α-GalCer/CD1d$^+$ iNKT cells on the indicated days after intraperitoneal injection of α-GalCer or OCH. One day after α-GalCer or OCH injection, both cell surface and intracellular expression of the indicated molecules were analyzed in electronically gated intracellular Vβ2/7/8$^+$ iNKT cells. The analysis gates are indicated by the gray line in dot plot panels. Bold lines indicate the staining with the respective mAb, and the thin lines indicate the staining with isotype-matched control Ig. Similar results were obtained from 3 independent experiments. (B) Existence of a cell population expressing intracellular α-GalCer/CD1d–specific TCR 1 day after α-GalCer injection. Liver MNCs were intracellularly stained with α-GalCer–loaded recombinant soluble dimeric mouse CD1d:Ig and PE-conjugated anti–mouse IgG1 mAb, or PE-conjugated anti–mouse IgG1 mAb together with FITC-conjugated anti-NK1.1 mAb, 1 day after α-GalCer injection. Quadrant gates were set by staining with FITC-conjugated isotype-matched control and PE-conjugated anti–mouse IgG1 mAb.

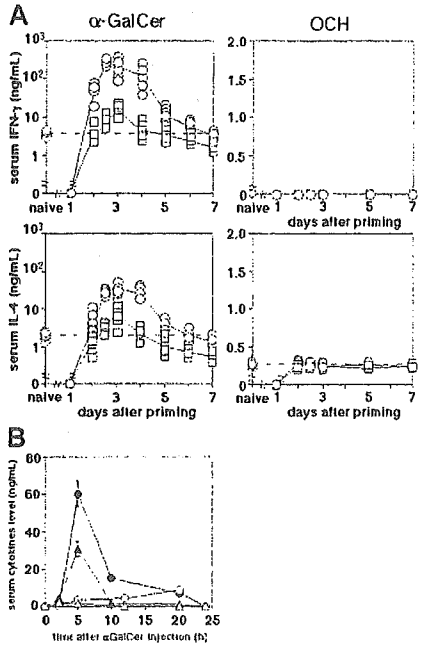

Figure 2. Augmented serum IFN-γ and IL-4 following α-GalCer treatment in OCH-primed mice. (A) Mice were primed with intraperitoneal injection of α-GalCer (□) or OCH (○) and then boosted with α-GalCer or OCH on the indicated day. Serum samples were obtained from 3 to 10 mice in each group 5 hours after the boost or the priming. Serum IFN-γ and IL-4 levels of primed naive mice were indicated on the y-axis (◇), and the dotted horizontal line in each panel shows the mean level of the primary response. Serum IFN-γ or IL-4 in the vehicle-injected mice were not detectable (data not shown). (B) Kinetics of serum IFN-γ (circles) and IL-4 (triangles) levels following α-GalCer boost of vehicle-primed (open symbols) or OCH-primed (closed symbols) mice on day 2.5. Data are represented as the mean ± SD of 5 mice in each group. Similar results were obtained from 3 independent experiments.

receptors by α-GalCer or OCH priming in IFN-γ$^{-/-}$ mice or in anti–IFN-γ mAb– and/or anti–IL-4 mAb–treated WT mice (data not shown). Taken together, these results indicated that priming of iNKT cells with TCR ligands resulted in a dramatic modulation of not only TCR and NK1.1 but also CD28 and inhibitory or activating NK-cell receptors on their surface, and this modulation was independent of IFN-γ or IL-4 production.

Augmented recall responses of OCH-primed iNKT cells to α-GalCer in vivo

Since the modulation of surface receptors on iNKT cells by Ag priming might modify iNKT-cell responses to subsequent Ag challenge, we next examined the responses of α-GalCer– or OCH-primed mice to secondary α-GalCer or OCH administration. We measured serum IFN-γ and IL-4 5 hours after α-GalCer or OCH injection to avoid the contribution of NK cells, since it has been previously reported that NK cells are activated after iNKT-cell activation and contribute significantly to IFN-γ production within 12 hours after α-GalCer injection.[16,31] Of interest, serum IFN-γ and IL-4 levels were dramatically increased (10-30 fold) by secondary α-GalCer injection 2 to 4 days after OCH priming compared with primary α-GalCer injection (Figure 2A). By contrast, serum IFN-γ and IL-4 levels were only slightly increased by secondary α-GalCer injection in α-GalCer–primed mice compared with primary α-GalCer injection (Figure 2A). Very little serum IFN-γ and IL-4 were detected in mice injected with α-GalCer 1 day after α-GalCer or OCH priming, possibly due to the initial internalization of TCR in iNKT cells. OCH administration after α-GalCer or OCH priming did not augment serum IL-4 levels compared with primary administration of OCH, and serum IFN-γ was never detected (Figure 2A). We also examined the kinetics of serum IFN-γ and IL-4 induction by α-GalCer injection 2.5 days after OCH priming. Both IFN-γ and IL-4 levels were dramatically increased by the OCH priming and peaked at 5 hours after secondary α-GalCer injection (Figure 2B).

We next examined the α-GalCer–induced cytotoxic activity and antitumor effect in α-GalCer– or OCH-primed mice. OCH priming markedly augmented the α-GalCer–induced cytotoxic activities of liver and spleen MNCs against either NK-cell–sensitive YAC-1 or NK-cell–resistant P815 target cells compared with priming with the vehicle (Figure 3A). However, the iNKT-cell proportions in MNCs were similar among the groups when the mice were boosted by secondary α-GalCer injection (Table 1). In contrast, α-GalCer priming did not significantly augment the secondary α-GalCer–induced cytotoxicity (Figure 3A). Moreover, α-GalCer administration 2.5 days after OCH priming markedly augmented the antimetastatic effect against B16 melanoma compared with other prime/boost regimens (eg, α-GalCer/α-GalCer; Figure 3B). These results indicated that iNKT cells were hyperresponsive to secondary α-GalCer stimulation 2 to 3 days after OCH priming in vivo, resulting in a dramatic augmentation of effector functions, including IFN-γ and IL-4 production, cytotoxicity, and antitumor effect.

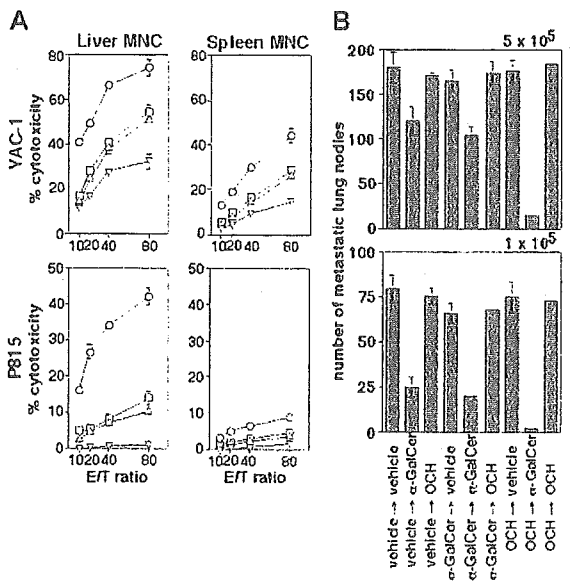

Figure 3. Induction of cytotoxic activity and antimetastatic effect by priming and boosting with α-GalCer and OCH. (A) Cytotoxic activity of liver and spleen MNCs was tested against NK-cell–sensitive YAC-1 cells or NK-cell–resistant P815 cells 24 hours after α-GalCer injection into mice primed 2.5 days earlier with vehicle (△), αGalCer (□), or OCH (○). Control mice were primed and boosted with vehicle (▽). Proportion of iNKT cells (%) in respective MNC populations at the time of boosting injection is indicated in Table 1. Data are represented as the mean ± SD of triplicate samples. Similar results were obtained from 3 independent experiments. E/T indicates effector-to-target ratio. (B) Antimetastatic effect. Mice were primed and boosted with α-GalCer, OCH, or vehicle on days −3 and 0 as indicated. Then, the indicated number of B16 melanoma cells were intravenously inoculated into the mice 2 hours after the boost. On day 14, the number of tumor metastatic colonies in the lungs was counted. Data are represented as the mean ± SD of 5 mice in each group. Similar results were obtained from 3 independent experiments.

Table 1. Proportion of iNKT cells in respective MNC populations at the time of boosting injection

	Liver MNCs, %	Spleen MNCs, %
Vehicle primed	22.7 ± 4.4	1.7 ± 0.8
α-GalCer primed	24.5 ± 3.4	3.3 ± 1.8
OCH primed	23.6 ± 5.1	2.5 ± 1.5

Suppression of α-GalCer–induced iNKT-cell activation by Qa-1^b and CD94/NKG2A interaction

To evaluate the priming effects more precisely, spleen MNCs were periodically isolated from naive, α-GalCer–primed, or OCH-primed mice and then stimulated with α-GalCer or OCH in vitro (Figure 4A). At 24 hours after the in vitro stimulation with α-GalCer or OCH, spleen MNCs from naive mice did not produce either IFN-γ or IL-4 at detectable levels, but by contrast spleen MNCs from α-GalCer– or OCH-primed mice produced substantial amounts of IFN-γ and IL-4 (Figure 4A). Maximal cytokine secretion was obtained from spleen MNCs isolated 2.5 days after priming. Consistent with the in vivo data (Figure 2), OCH-primed spleen MNCs secreted greater amounts of cytokines compared with α-GalCer–primed spleen MNCs. At 48 to 72 hours after the in vitro stimulation, naive splenic MNCs produced substantial amounts of IFN-γ and IL-4 in response to α-GalCer, but the OCH-primed MNCs still produced increased levels of both IFN-γ and IL-4 in response to α-GalCer restimulation compared with naive or α-GalCer–primed MNCs (data not shown). These results indicated that OCH priming sensitized iNKT cells to secondary α-GalCer stimulation more effectively than α-GalCer priming.

We next explored the mechanism by which OCH or α-GalCer priming sensitized iNKT cells to α-GalCer restimulation. We first examined whether the CD94/NKG2 inhibitory receptor might regulate the hyperresponsiveness of iNKT cells, since CD94/NKG2 was down-modulated on the sensitized iNKT cells 2 to 3 days after α-GalCer or OCH priming (Figure 1). Blockade of the CD94/NKG2 and Qa-1^b interaction by Fab fragments of anti-NKG2 mAb or anti–Qa-1^b mAb markedly enhanced IFN-γ and IL-4 production by α-GalCer–primed MNCs in response to restimulation in vitro with α-GalCer (Figure 4B). Albeit to a lesser extent, IFN-γ and IL-4 production by OCH-primed or naive MNCs was also significantly enhanced by the blockade of Qa-1^b or CD94/NKG2. Notably, while α-GalCer–primed MNCs produced lower levels of IFN-γ and IL-4 than OCH-primed MNCs in response to α-GalCer restimulation in vivo, this difference was abrogated by the blockade of Qa-1^b or CD94/NKG2. The contribution of activating CD94/NKG2C/E NK-cell receptors may be negligible, since blockade of the Qa-1^b–CD94/NKG2 interaction did not inhibit cytokine production by α-GalCer–activated iNKT cells in all cocultures, even if anti-NKG2 mAb or anti–Qa-1^b mAb inhibited the function of activating CD94/NKG2C/E. Blockade of the CD80/CD86 interaction with CD28 abolished the cytokine production by naive or primed MNCs, irrespective of Qa-1^b or CD94/NKG2 blockade. These results indicated that the Qa-1^b and CD94/NKG2 interaction suppressed the TCR- and CD28-mediated activation of iNKT cells by α-GalCer, especially when the iNKT cells had first been primed with α-GalCer.

We also examined the impact of OCH or α-GalCer priming on antigen-presenting cells (APCs) by coculturing of purified iNKT cells and purified splenic DCs separately isolated 2.5 days after priming with α-GalCer, OCH, or vehicle (Figure 4C). Neither IFN-γ nor IL-4 was detected when iNKT cells were cocultured with any DCs in the absence of α-GalCer (data not shown). Notably, α-GalCer–primed DCs induced significantly lower levels of IFN-γ and IL-4 production by vehicle-primed iNKT cells compared with vehicle- or OCH-primed DCs. Of importance, this difference was abrogated by the blockade of CD94/NKG2. Moreover, OCH-primed iNKT cells produced significantly higher levels of IFN-γ and IL-4 compared with vehicle- or α-GalCer–primed iNKT cells. Again, the difference of cytokine production between OCH-primed and α-GalCer–primed iNKT cells was abrogated by CD94/NKG2 blockade. Significantly higher levels of IFN-γ and IL-4 were attained by both types of primed iNKT cells compared with vehicle-primed iNKT cells. A similar level (approximately 200 pg/mL) of IL-12 p40 was detected in the supernatants of all

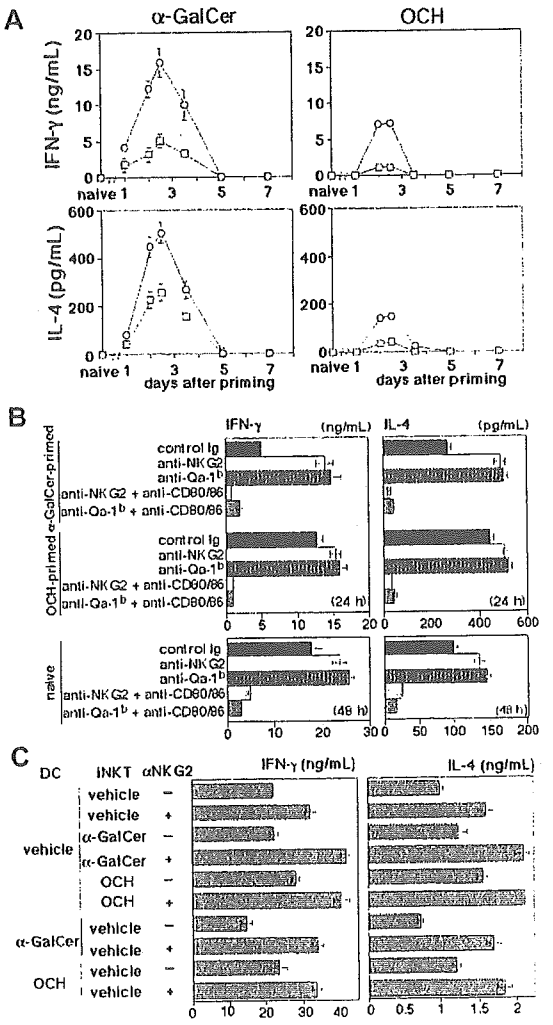

Figure 4. NKG2 and CD28 regulate activation of naive or primed iNKT cells by α-GalCer. (A) Mice were primed with intraperitoneal injection of α-GalCer (□) or OCH (○). Splenic MNCs were prepared on the indicated days after priming and stimulated with α-GalCer or OCH in vitro for 24 hours. Data are represented as the mean ± SD of triplicate wells. Similar results were obtained from 3 independent experiments. (B) Mice were primed with intraperitoneal injection of α-GalCer, OCH, or vehicle on day −2.5. Then, splenic MNCs were prepared on day 0 and stimulated with α-GalCer in vitro for 24 or 48 hours in the presence or absence of the indicated mAbs. Data are represented as the mean ± SD of triplicate wells. Similar results were obtained from 3 independent experiments. (C) Liver iNKT cells and splenic DCs were isolated from naive mice or primed with α-GalCer or OCH 2.5 days before and then cocultured with α-GalCer for 48 hours in the presence or absence of anti-NKG2 mAb. Data are represented as the mean ± SD of triplicate wells. Similar results were obtained from 2 independent experiments.

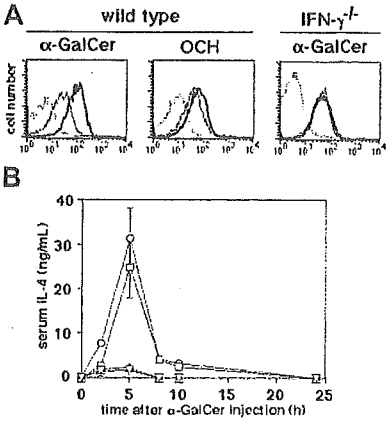

Figure 5. IFN-γ–induced Qa-1^b inhibits reactivation of α-GalCer–primed iNKT cells by α-GalCer. (A) Qa-1^b expression on splenic MNCs isolated from WT and IFN-γ$^{-/-}$ mice was analyzed 2.5 days after intraperitoneal administration of α-GalCer or OCH. Thin lines indicate the staining of MNCs from vehicle-treated mice with anti–Qa-1^b mAb; bold lines, the staining of MNCs from α-GalCer– or OCH-treated mice with anti–Qa-1^b mAb; and dotted lines, the staining with isotype-matched control Ig. Similar results were obtained from 3 independent experiments. (B) Kinetics of serum IL-4 induction after α-GalCer injection into vehicle-primed wild-type mice (▽), vehicle-primed IFN-γ$^{-/-}$ mice (△), α-GalCer–primed IFN-γ$^{-/-}$ mice (□), or OCH-primed IFN-γ$^{-/-}$ mice (○). Priming was performed 2.5 days before. Serum IL-4 was not detectable in the vehicle-injected mice (data not shown). Data are represented as the mean ± SD of 5 mice in each group. Similar results were obtained from 3 independent experiments.

cocultures (data not shown), which suggested that DC function was not impaired by α-GalCer or OCH priming. These results suggested that the recall responses of iNKT cells in α-GalCer–primed mice were more strictly regulated by Qa-1^b and CD94/NKG2-mediated suppression than in naive or OCH-primed mice. Consistent with this notion, Qa-1^b expression on splenic MNCs was markedly up-regulated in α-GalCer–primed mice compared with naive or OCH-primed mice (Figure 5A).

IFN-γ–induced Qa-1^b expression negatively regulates recall NKT-cell responses in vivo

Although iNKT cells primed with α-GalCer strongly up-regulated the Qa-1^b expression on splenic MNCs, those primed with OCH did so only weakly (Figure 5A). Notably, the α-GalCer–induced Qa-1^b up-regulation was not observed in IFN-γ$^{-/-}$ mice (Figure 5A). Moreover, α-GalCer priming increased the secondary α-GalCer–induced serum IL-4 to a level comparable with that induced by OCH priming in IFN-γ$^{-/-}$ mice (Figure 5B). These results indicated that IFN-γ induced by α-GalCer priming was responsible for Qa-1^b up-regulation, which in turn resulted in CD94/NKG2-mediated suppression of recall iNKT-cell response in α-GalCer–primed mice.

We finally evaluated whether the blockade of CD94/NKG2 could augment the α-GalCer–induced iNKT-cell function in α-GalCer–primed mice. The in vivo treatment with anti-NKG2 mAb alone did not induce cytokine production or cytotoxicity and did not deplete NK cells or iNKT cells (data not shown). The CD94/NKG2 blockade dramatically increased α-GalCer–induced serum IFN-γ and IL-4 levels, particularly in α-GalCer–primed mice (Figure 6A). It was notable that high levels of serum IFN-γ and IL-4 were inducible 10 days after α-GalCer priming if CD94/NKG2 was blocked at the time of boosting. Moreover, the CD94/NKG2 blockade also significantly augmented the α-GalCer–induced cytotoxicity of liver and spleen MNCs and the antimetastatic effect of treatment, particularly in α-GalCer–primed mice (Figure 6B-C). Even if anti-NKG2 mAb possibly inhibited the function of activating CD94/NKG2C/E, the contribution of activating CD94/NKG2C/E NK-cell receptors may be negligible, since blockade of the Qa-1^b–CD94/NKG2 interaction did not inhibit

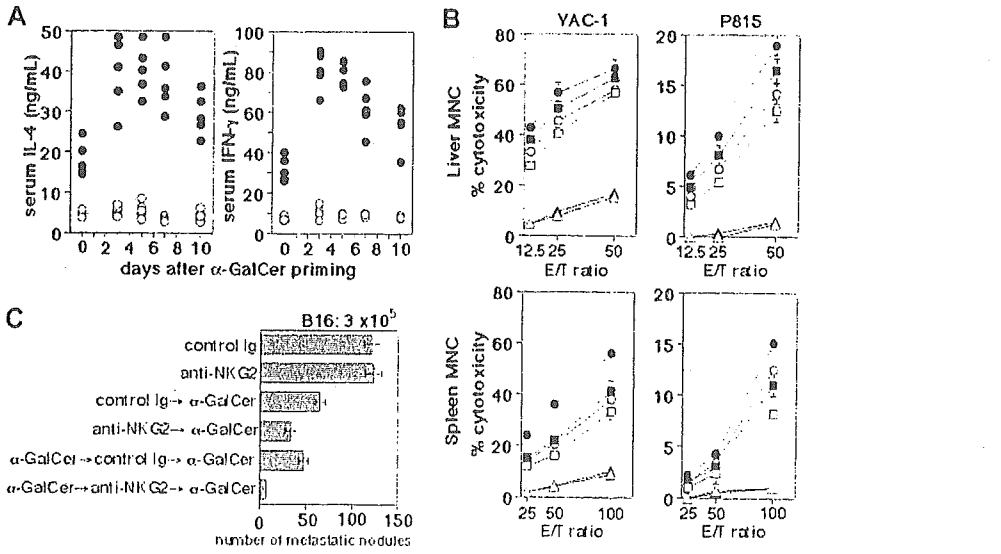

Figure 6. Blockade of NKG2 enhances activation of naive and α-GalCer–primed iNKT cells by α-GalCer in vivo. (A) Mice were primed with α-GalCer on day 0 and then boosted with α-GalCer on the indicated day. Anti-NKG2 mAb (●) or control Ig (○) was administered 2 days before the boost. Serum samples were obtained 5 hours after the boost. The mice indicated on day 0 were treated once with α-GalCer injection on day 0. (B) Cytotoxic activity of liver and spleen MNCs was tested against NK-sensitive YAC-1 cells and NK-resistant P815 cells 24 hours after the last α-GalCer injection. Mice were intraperitoneally injected with α-GalCer on day 0 (squares) or days −3 and 0 (circles), or injected with vehicle on days −3 and 0 (triangles), and intraperitoneally administered with anti-NKG2 mAb (closed symbols) or control Ig (open symbols) on day −2. Data are represented as the mean ± SD of triplicate samples. Similar results were obtained from 3 independent experiments. (C) Antimetastatic effect. Mice were intraperitoneally injected with α-GalCer on day 0 or days −3 and 0, and then intravenously inoculated with 3 × 10^5 B16 melanoma cells 2 hours later. Anti-NKG2 mAb or control Ig was intraperitoneally administered on day −2. On day 14, the number of tumor colonies in the lungs was counted under a dissecting microscope. Data are represented as the mean ± SD of 5 to 8 mice in each group. Similar results were obtained from 3 independent experiments.

cytokine production, cytotoxic activity, or the antimetastatic effect caused by the α-GalCer injection. These results indicated that the iNKT-cell activation by α-GalCer was limited by CD94/NKG2-mediated suppression and blockade of CD94/NKG2 could significantly improve the antitumor effect of a secondary α-GalCer treatment.

Discussion

In this study, we have shown that activation of iNKT cells is critically regulated by CD94/NKG2. In addition to TCR and CD28, naive iNKT cells express activating (NK1.1, NKG2D, and Ly49D) or inhibitory (CD94/NKG2 and Ly49A/C/I/G2) NK-cell receptors. All of these cell surface receptors were rapidly down-modulated upon priming of iNKT cells with their TCR ligands (α-GalCer or OCH). Two to 3 days after the priming, iNKT cells re-expressed TCR and CD28 on their surface, but CD94/NKG2 and Ly49 remained down-modulated. This pattern of expression enabled the primed iNKT cells to produce a larger amount of cytokines upon secondary stimulation with α-GalCer. Of interest, OCH was superior to α-GalCer in priming iNKT cells for a secondary response to α-GalCer, resulting in a markedly enhanced antimetastatic effect. We found that IFN-γ induced by α-GalCer priming up-regulated Qa-1^b, which in turn suppressed the secondary iNKT-cell activation via CD94/NKG2. Thus, the blockade of CD94/NKG2 markedly enhanced the antimetastatic effect of α-GalCer after α-GalCer priming. These findings revealed a negative feedback regulation of iNKT-cell activation by IFN-γ–inducible Qa-1^b and provided a novel strategy to improve the antimetastatic effect of α-GalCer by priming with OCH or by blocking CD94/NKG2-mediated suppression.

It was unexpected that OCH was far more effective than α-GalCer in priming the secondary iNKT-cell responses to α-GalCer, since OCH and α-GalCer similarly modulated iNKT-cell surface receptors and OCH was rather inferior to α-GalCer in expanding iNKT cells upon priming (data not shown) as recently reported.[6,9] We hypothesized that IFN-γ produced by iNKT cells upon priming with α-GalCer might be responsible for this difference, since OCH did not induce IFN-γ production in vivo. We found that α-GalCer priming up-regulated the expression of Qa-1^b in an IFN-γ–dependent manner, which suppressed iNKT-cell activation in response to secondary α-GalCer stimulation in vitro and in vivo. Qa-1^b is an MHC class Ib molecule broadly expressed on leukocytes and it predominantly presents a canonical signal peptide of classical MHC class Ia molecules, called Qa-1 determinant modifier (Qdm), in a transporter associated with antigen presentation (TAP)–dependent manner, thereby indirectly representing cellular MHC class Ia levels.[32,33] The up-regulation of Qa-1^b expression by IFN-γ might be due to increased transcription of *Qa-1^b* and/or increased TAP-mediated loading of Qdm onto Qa-1^b. The Qdm/Qa-1^b complex is recognized by inhibitory CD94/NKG2A and activating CD94/NKG2C or E receptors.[21-23] The CD94/NKG2 receptors expressed on naive and primed iNKT cells were predominantly CD94/NKG2A as estimated by staining with an NKG2A-specific mAb as previously reported.[22] It has been shown that CD94/NKG2A expressed on NK cells and $CD8^+$ T cells suppressed their activation.[34] However, our present results are the first indication that iNKT-cell activation is critically regulated by CD94/NKG2A. Similarly, inhibitory Ly49 receptors, which recognize MHC class Ia molecules directly, have been reported to suppress α-GalCer–induced iNKT-cell activation.[30,35] Since CD94/NKG2A is more frequently expressed on iNKT cells than Ly49, it may play a more dominant role in regulating iNKT-cell activation. The IFN-γ–mediated Qa-1^b up-regulation may be a negative feedback mechanism to maintain self-tolerance of iNKT cells and avoid a pathogenic effect of iNKT cells.[36-39] It will be interesting to explore the iNKT-cell functions in Qa-1^b–deficient[40] or CD94-deficient[22] mice in future studies.

Consistent with recent reports,[18-20] we observed a rapid down-modulation of TCR and NK1.1 on the surface of iNKT cells upon priming with their TCR ligands, which mostly accounted for the apparent disappearance of iNKT cells. However, intracellular staining 1 day after α-GalCer priming demonstrated a 20% to 30% reduction of iNKT-cell numbers compared with untreated mice (data not shown), and some annexin V–positive iNKT cells were detected in the liver and spleen promptly after α-GalCer injection as we reported previously.[16] Therefore, some minor fraction of iNKT cells appeared to be susceptible to AICD upon α-GalCer priming. A significant increase of CD94/$NKG2^+$ iNKT cells after α-GalCer priming suggested that these cells were more resistant to AICD than CD94/$NKG2^-$ iNKT cells. This preferential survival and/or expansion of CD94/$NKG2^+$ iNKT cells might be at least partly responsible for the higher sensitivity of primed iNKT cells to Qa-1^b and CD94/NKG2-mediated suppression.

We and others have recently shown that the expansion of iNKT cells is maximal 3 days after α-GalCer priming and then iNKT-cell numbers gradually return to normal levels by homeostatic mechanisms within 7 to 10 days.[9,18-20] This is consistent with the kinetics of recall responses of α-GalCer– or OCH-primed mice to α-GalCer, suggesting that the enhanced secondary responses were mainly due to expansion of iNKT cells after priming. However, the enhanced secondary responses were mostly maintained up to 10 days after α-GalCer priming if CD94/NKG2-mediated suppression was blocked at the secondary α-GalCer stimulation. This suggests that the primed iNKT cells with a high capacity to produce cytokines upon restimulation persist (typical of effector/ memory T cells), although they are under a strict regulation by CD94/NKG2A-mediated suppression.

A recent study has shown that the recognition of α-GalCer analogues was influenced by the TCR Vβ repertoires of iNKT cells. OCH was preferentially recognized by $V\beta8^+$ iNKT cells, which also have a higher avidity for α-GalCer than $V\beta7^+$ iNKT cells.[7,41] Thus, a preferential expansion of $V\beta8^+$ iNKT cells after OCH or α-GalCer priming might also be responsible for the enhanced responses of primed iNKT cells to α-GalCer restimulation in vitro and in vivo.

We have previously shown that α-GalCer administration into naive mice induces sustained IFN-γ production and cytotoxic activity, which were mediated by NK cells secondarily activated by IFN-γ derived from iNKT cells and IL-12 derived from DCs.[16,29,31] Thus, depletion of NK cells mostly abrogated the sustained α-GalCer response and consequently impaired the antimetastatic effect of α-GalCer. In contrast, α-GalCer administration into OCH-primed mice induced a greatly enhanced IFN-γ production at 5 hours but not at 16 to 20 hours, which was not reduced by NK-cell depletion (data not shown). This indicated that OCH priming mainly enhanced IFN-γ production by iNKT cells themselves, rather that secondary activated NK cells, upon the secondary α-GalCer stimulation. However, the markedly enhanced cytotoxic activity of liver and spleen MNCs 24 hours after α-GalCer boost in OCH-primed mice was mostly abrogated by NK-cell depletion (K.T., unpublished data, May 2004). In addition, the

significantly augmented antimetastatic effect of α-GalCer in OCH-primed mice was significantly inhibited by NK-cell depletion (K.T., unpublished data, May 2004). These data suggested that IFN-γ–activated NK cells were mainly responsible for the antimetastatic effect of α-GalCer in the OCH-primed mice. In this context, the CD94/NKG2 blockade might augment the antimetastatic effect of α-GalCer by enhancing the activation of not only iNKT cells but also NK cells, since NK cells also express CD94/NKG2A inhibitory receptors. Thus, blockade of the CD94/NKG2A suppressive pathway may be effective at either the induction or effector phase of the α-GalCer–induced antitumor effect.

The most notable finding of this study is that the antimetastatic effect of α-GalCer was greatly improved by the OCH-priming or the CD94/NKG2A blockade. OCH was a weak inducer of iNKT-cell expansion and IL-4 production but did not induce IFN-γ production or antimetastatic activity by itself.[6,7,9] However, OCH modulated iNKT-cell surface receptors as efficiently as α-GalCer. These OCH-primed iNKT cells produced a huge amount of IFN-γ upon secondary α-GalCer restimulation in vivo, resulting in a potent antimetastatic effect. The inability of OCH to induce IFN-γ was a beneficial property for priming secondary α-GalCer responses because IFN-γ down-regulated the secondary iNKT-cell responses by up-regulating Qa-1^b and thus CD94/NKG2A-mediated suppression. Recent studies have demonstrated quantitative and qualitative differences in the in vivo response of iNKT cells to distinct α-GalCer analogues, including OCH and β-GalCer.[9] Like OCH, in our preliminary experiments, priming with β-GalCer a26,[9] another weak iNKT-cell ligand inducing poor cytokine production, also potently enhanced iNKT-cell responses to α-GalCer restimulation (data not shown). α-GalCer and OCH have been shown to activate human Vα24 iNKT cells in a similar manner to murine Vα14 iNKT cells in vitro,[3,4] and α-GalCer is now in early clinical trials in cancer patients.[42,43] Therefore, priming with OCH may be a novel strategy to improve the therapeutic effect of α-GalCer in such patients. Further exploration of an α-GalCer analog with a better priming effect is also warranted. CD94/NKG2A blockade might be also applicable to improve the antitumor effect of α-GalCer in humans. In addition to an antitumor effect, α-GalCer has been shown to protect mice against infections and autoimmune diseases.[1-4,13,14] Therefore, the priming with OCH and the blockade of CD94/NKG2A may also be applicable to improve the therapeutic effect of α-GalCer in these diseases. However, it has also been shown that α-GalCer occasionally exacerbated autoimmune diseases, depending on the model and/or administration protocol.[44] Moreover, overactivation of iNKT cells can induce tissue pathologies.[36-39] Therefore, further studies are needed to determine the optimal prime/boost protocol or blockade of NK-cell receptors in iNKT-cell–targeting therapy for the safe treatment of tumor, infections, and autoimmune diseases.

Acknowledgment

We thank Lewis L. Lanier for reading the manuscript and helpful suggestions.

References

1. Bendelac A, Rivera MN, Park SH, Roark JH. Mouse CD1-specific NK1 T cells: development, specificity, and function. Annu Rev Immunol. 1997;15:535-562.
2. Godfrey DI, Hammond KJ, Poulton LD, Smyth MJ, Baxter AG. NKT cells: facts, functions and fallacies. Immunol Today. 2000;21:573-583.
3. Kronenberg M, Gapin L. The unconventional lifestyle of NKT cells. Nat Rev Immunol. 2002;2:557-568.
4. Taniguchi M, Harada M, Kojo S, Nakayama T, Wakao H. The regulatory role of Vα14 NKT cells in innate and acquired immune response. Annu Rev Immunol. 2003;21:483-513.
5. Kawano T, Cui J, Koezuka Y, et al. CD1d-restricted and TCR-mediated activation of Vα14 NKT cells by glycosylceramides. Science. 1997; 278:1626-1629.
6. Miyamoto K, Miyake S, Yamamura T. A synthetic glycolipid prevents autoimmune encephalomyelitis by inducing TH2 bias of natural killer T cells. Nature. 2001;413:531-534.
7. Stanic AK, Shashidharamurthy R, Bezbradica JS, et al. Another view of T cell antigen recognition: cooperative engagement of glycolipid antigens by Vα14Jα18 natural T(iNKT) cell receptor. J Immunol. 2003;171:4539-4551.
8. Ortaldo JR, Young HA, Winkler-Pickett RT, Bere EW Jr, Murphy WJ, Wiltrout RH. Dissociation of NKT stimulation, cytokine induction, and NK activation in vivo by the use of distinct TCR-binding ceramides. J Immunol. 2004;172:943-953.
9. Parekh VV, Singh AK, Wilson MT, et al. Quantitative and qualitative differences in the in vivo response of NKT cells to distinct α- and β-anomeric glycolipids. J Immunol. 2004;173:3693-3706.
10. Zhou D, Mattner J, Vantu III C, et al. Lysosomal glycosphingolipid recognition by NKT cells. Science. 2004;306:1786-1789.
11. Hayakawa Y, Takeda K, Yagita H, Van Kaer L, Saiki I, Okumura K. Differential regulation of Th1 and Th2 functions of NKT cells by CD28 and CD40 costimulatory pathways. J Immunol. 2001; 166:6012-6018.
12. Ikarashi Y, Mikami R, Bendelac A, et al. Dendritic cell maturation overrules H-2D-mediated natural killer T (NKT) cell inhibition: critical role for B7 in CD1d-dependent NKT cell interferon γ production. J Exp Med. 2001;194:1179-1186.
13. Smyth MJ, Godfrey DI. NKT cells and tumor immunity: a double-edged sword. Nat Immunol. 2000;1:459-460.
14. Smyth MJ, Crowe NY, Hayakawa Y, Takeda K, Yagita H, Godfrey DI. NKT cells: conductors of tumor immunity? Curr Opin Immunol. 2002;14: 165-171.
15. Eberl G, MacDonald HR. Rapid death and regeneration of NKT cells in anti-CD3ε- or IL-12-treated mice: a major role for bone marrow in NKT cell homeostasis. Immunity. 1998;9:345-353.
16. Hayakawa Y, Takeda K, Yagita H, et al. Critical contribution of IFN-γ and NK cells, but not perforin-mediated cytotoxicity, to anti-metastatic effect of α-galactosylceramide. Eur J Immunol. 2001;31:1720-1727.
17. Matsuda JL, Naidenko OV, Gapin L, et al. Tracking the response of natural killer T cells to a glycolipid antigen using CD1d tetramers. J Exp Med. 2000;192:741-754.
18. Wilson MT, Johansson C, Olivares-Villagómez D, et al. The response of natural killer T cells to glycolipid antigens is characterized by surface receptor down-modulation and expansion. Proc Natl Acad Sci U S A. 2003;100:10913-10918.
19. Crowe NY, Uldrich AP, Kyparissoudis K, et al. Glycolipid antigen drives rapid expansion and sustained cytokine production by NK T cells. J Immunol. 2003;171:4020-4027.
20. Harada M, Seino K, Wakao H, et al. Down-regulation of the invariant Vα14 antigen receptor in NKT cells upon activation. Int Immunol. 2004;16:241-247.
21. Vance RE, Jamieson AM, Raulet DH. Recognition of the class Ib molecule Qa-1^b by putative activating receptors CD94/NKG2C and CD94/NKG2E on mouse natural killer cells. J Exp Med. 1999; 190:1801-1812.
22. Vance RE, Jamieson AM, Cado D, Raulet DH. Implications of CD94 deficiency and monoallelic NKG2A expression for natural killer cell development and repertoire formation. Proc Natl Acad Sci U S A. 2002;99:868-873.
23. Vance RE, Kraft JR, Altman JD, Jensen PE, Raulet DH. Mouse CD94/NKG2A is a natural killer cell receptor for the nonclassical major histocompatibility complex (MHC) class I molecule Qa-1^b. J Exp Med. 1998;188:1841-1848.
24. Tagawa Y, Sekikawa K, Iwakura Y. Suppression of concanavalin A-induced hepatitis in IFN-γ$^{-/-}$ mice, but not in TNF-α$^{-/-}$ mice: role for IFN-γ in activating apoptosis of hepatocytes. J Immunol. 1997;159:1418-1428.
25. Ogasawara K, Hamerman JA, Hsin H, et al. Impairment of NK cell function by NKG2D modulation in NOD mice. Immunity. 2003;18:41-51.
26. Tajima A, Tanaka T, Ebata T, et al. Blastocyst MHC, a putative murine homologue of HLA-G, protects TAP-deficient tumor cells from natural killer cell-mediated rejection in vivo. J Immunol. 2003;171:1715-1721.
27. Ruedl C, Rieser C, Bock G, Wick G, Wolf H. Phenotypic and functional characterization of CD11c$^+$ dendritic cell population in mouse Peyer's patches. Eur J Immunol. 1996;26:1801-1806.
28. Maldonado-Lopez R, De Smedt T, Michel P, et al. CD8α$^+$ and CD8α$^-$ subclasses of dendritic cells direct the development of distinct T helper cells in vivo. J Exp Med. 1999;189:587-592.
29. Kitamura H, Iwakabe K, Yahata T, et al. The natural killer T (NKT) cell ligand α-galactosylceramide demonstrates its immunopotentiating effect by inducing interleukin (IL)-12 production by dendritic cells and IL-12 receptor expression on NKT cells. J Exp Med. 1999;189:1121-1128.

30. Hayakawa Y, Berzins SP, Crowe NY, Godfrey DI, Smyth MJ. Antigen-induced tolerance by intrathymic modulation of self-recognizing inhibitory receptors. Nat Immunol. 2004;5:590-596.

31. Carnaud C, Lee D, Donnars O, et al. Cross-talk between cells of the innate immune system: NKT cells rapidly activate NK cells. J Immunol. 1999; 163:4647-4650.

32. Soloski MJ, DeCloux A, Aldrich CJ, Forman J. Structural and functional characteristics of the class Ib molecule, Qa-1. Immunol Rev. 1995;147: 67-89.

33. Aldrich CJ, DeCloux A, Woods AS, Cotter RJ, Soloski MJ, Forman J. Identification of a Tap-dependent leader peptide recognized by alloreactive T cells specific for a class Ib antigen. Cell. 1994;79: 649-658.

34. Vivier E, Anfossi N. Inhibitory NK-cell receptors on T cells: witness of the past, actors of the future. Nat Rev Immunol. 2004;4:190-198.

35. Maeda M, Lohwasser S, Yamamura T, Takei F. Regulation of NKT cells by Ly49: analysis of primary NKT cells and generation of NKT cell line. J Immunol. 2001;167:4180-4186.

36. Takeda K, Hayakawa Y, Van Kaer L, Matsuda H, Yagita H, Okumura K. Critical contribution of liver natural killer T cells to a murine model of hepatitis. Proc Natl Acad Sci U S A. 2000;97:5498-5503.

37. Osman Y, Kawamura T, Naito T, et al. Activation of hepatic NKT cells and subsequent liver injury following administration of α-galactosylceramide. Eur J Immunol. 2000;30:1919-1928.

38. Ito K, Karasawa T, Kawano T, et al. Involvement of decidual Vα14 NKT cells in abortion. Proc Natl Acad Sci U S A. 2000;97:740-744.

39. Tupin E, Nicoletti A, Elhage R, et al. CD1d-dependent activation of NKT cells aggravates atherosclerosis. J Exp Med. 2004;199:417-422.

40. Hu D, Ikizawa K, Lu L, Sanchirico ME, Shinohara ML, Cantor H. Analysis of regulatory CD8 T cells in Qa-1-deficient mice. Nat Immunol. 2004;5:516-523.

41. Schümann J, Voyle RB, Wei BY, MacDonald HR. Influence of the TCR Vβ domain on the avidity of CD1d:α-galactosylceramide binding by invariant Vα 14 NKT cells. J Immunol. 2003;170:5815-5819.

42. Giaccone G, Punt CJ, Ando Y, et al. A phase I study of the natural killer T-cell ligand α-galactosylceramide (KRN7000) in patients with solid tumors. Clin Cancer Res. 2002;8:3702-3709.

43. Nieda M, Okai M, Tazbirkova A, et al. Therapeutic activation of $Vα24^+Vβ11^+$ NKT cells in human subjects results in highly coordinated secondary activation of acquired and innate immunity. Blood. 2004;103:383-389.

44. Mars LT, Novak J, Liblau RS, Lehuen A. Therapeutic manipulation of iNKT cells in autoimmunity: modes of action and potent risks. Trends Immunol. 2004;25:471-476.